

# PL-embedding the dual of two Jordan curves into $\mathbb{S}^3$ by an $O(n^2)$ -algorithm \*

Sóstenes L. Lins and Ricardo N. Machado

April 20, 2022

## Abstract

Let be given a *colored 3-pseudo-triangulation*  $\mathcal{H}^*$  with  $n$  tetrahedra. Colored means that each tetrahedron have vertices distinctively colored 0,1,2,3. In a *pseudo* 3-triangulation the intersection of simplices might be subsets of simplices of smaller dimensions (faces), instead of a single maximal face, as for true triangulations. If  $\mathcal{H}^*$  is the dual of a cell 3-complex induced (in an specific way to be made clear) by a pair of Jordan curves with  $2n$  transversal crossings, then we show that the induced 3-manifold  $|\mathcal{H}^*|$  is  $\mathbb{S}^3$  and we make available an  $O(n^2)$ -algorithm to produce a PL-embedding ([15]) of  $\mathcal{H}^*$  into  $\mathbb{S}^3$ . This bound is rather surprising because such PL-embeddings are often of exponential size. This work is the first step towards obtaining, via an  $O(n^2)$ -algorithm, a framed link presentation inducing the same closed orientable 3-manifold as the one given by a colored pseudo-triangulation. Previous work on this topic appear in <http://arxiv.org/abs/1212.0827>, [12], <http://arxiv.org/abs/1212.0826>, [13] and <http://arxiv.org/abs/1211.1953>, [14]. However, the exposition and the new proofs of this paper are meant to be entirely self-contained.

## 1 Introduction

The subject of this paper is motivated by the following problem: given a triangulated closed, connected, orientable 3-manifold  $\mathbb{R}^3$ , how to obtain by a polynomial algorithm a *blackboard-framed link presentation* inducing  $\mathbb{R}^3$ . This is one of the most basic open problems in 3-manifold topology: there are two main languages to present a specific 3-manifold. The triangulation based presentations (triangulations, Heegaard diagrams, gems, special spines, etc) and the framed link presentations (various types of decorated links which yield the 3-manifold as a recipe for surgery on  $\mathbb{S}^3$ ). Going from the second type presentation to a first type one is straightforward by a linear algorithm, see Section 2 of <http://arxiv.org/abs/1305.5590>, [11]. However there is no known polynomial algorithm to go from the first to the second. This paper starts to remedy this situation.

A blackboard-framed link is in 1-1 correspondence with a *blink*, which is simply a plane graph with an arbitrary bipartition of the edges set into black and gray edges. For a recent combinatorially oriented account about how a blink induces a 3-manifold, see <http://arxiv.org/abs/1305.4540>, [10]. The blink of the bottom part of Fig. 1 provides a solution for a problem left open in <http://arxiv.org/arXiv:math/0702057>, [4]. Even though the general problem remains

---

\*2010 Mathematics Subject Classification: 57M25 and 57Q15 (primary), 57M27 and 57M15 (secondary)

unconquered, substantial advances were possible and, in practice, it permits to find by an  $O(n^2)$ -algorithm a blink presentation inducing the same 3-manifold as a given gem. From here on we concentrate in producing an embedding into  $\mathbb{S}^3$  of a  $J^2$ -gem. This result is used as a central important lemma in finding the blink equivalent to a gem, which is the subject of subsequent papers currently being polished.

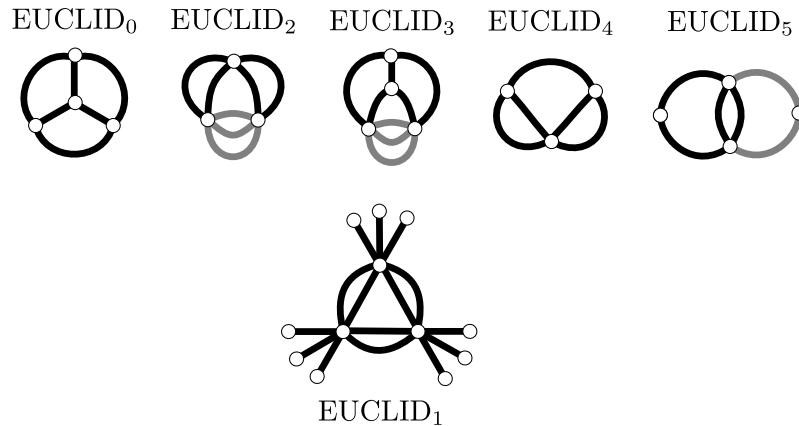


Figure 1: The discovery of a blink for  $\text{EUCLID}_1$ , solving an open problem left in page 117 of [4]: of the six euclidean 3-manifolds only  $\text{EUCLID}_1$  did not have a blink presentation. To find this blink it is necessary to develop and understanding some deep geometric properties of gems, as we start doing in in this paper. The blink presentation for  $\text{EUCLID}_1$  was obtained in this way.

## 1.1 $J^2$ -gems

A  $J^2$ -gem is a 4-regular, 4-edge-colored planar graph  $\mathcal{H}$  obtained from the intersection pattern of two Jordan curves  $X$  and  $Y$  with  $2n$  transversal crossings. These crossings define consecutive segments of  $X$  alternatively inside  $Y$  and outside  $Y$ . Color the first type 2 and the second type 3. The crossings also define consecutive segments of  $Y$  alternatively inside  $X$  and outside  $X$ . Color the first type 0 and the second type 1. This defines a 4-regular 4-edge-colored graph  $\mathcal{H}$  where the vertices are the crossings and the edges are the colored colored segments, see Fig. 2.

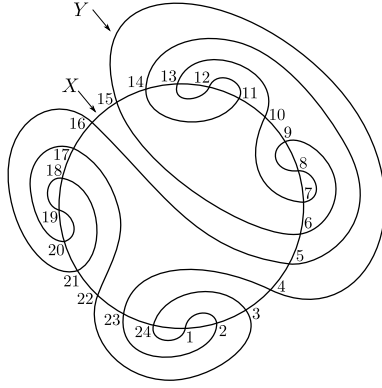


Figure 2: How to interpret a pattern formed by two  $2n$ -crossing Jordan curves as a gem: start labeling the crossings of  $X$  in consecutively in a counterclockwise way so that edge linking 1 to 2 is of color 2 which alternates with color 3. Let the segments of  $Y$  internal to  $X$  be colored 0 and the ones external to  $X$  be colored 1. The result is, by definition, a  $J^2$ -gem.

Let  $\mathcal{H}^*$  be the 3-dimensional abstract 3-complex formed by taking a set of vertex colored tetrahedra in 1–1 correspondence with the set of vertices of  $\mathcal{H}$ ,  $V(\mathcal{H})$ , so that each tetrahedra has vertices of colors 0,1,2,3. This vertex coloring induces a face coloring of the triangular faces of the tetrahedron: color  $i$  the face opposite to the vertex colored  $i$ . For each  $i$ -colored edge of  $\mathcal{H}$  with ends  $u$  and  $v$  paste the corresponding tetrahedra  $\nabla_u$  and  $\nabla_v$  so as to paste the two triangular faces that do not contain a vertex of color  $i$  in such a way as to match vertices of the other three colors. We show that the topological space  $|K|$  induced by  $\mathcal{H}^*$  is  $\mathbb{S}^3$ . Moreover we describe an  $O(n^2)$ -algorithm to make available a PL-embedding ([15]) of  $\mathcal{H}^*$  into  $\mathbb{S}^3$ . We get explicit coordinates in  $\mathbb{S}^3$  for the 0-simplices and the  $p$ -simplices ( $p \in \{1, 2, 3\}$ ) become linear simplices in the spherical geometry. For basic topological definitions we refer to the lucid book by Stillwell [16].

## 1.2 Gems and their duals

A  $(3+1)$ -graph  $\mathcal{H}$  is a connected regular graph of degree 4 where to each vertex there are four incident differently colored edges in the color set  $\{0, 1, 2, 3\}$ . For  $I \subseteq \{0, 1, 2, 3\}$ , an  $I$ -residue is a component of the subgraph induced by the  $I$ -colored edges. Denote by  $v(\mathcal{H})$  the number of 0-residues (vertices) of  $\mathcal{H}$ . For  $0 \leq i < j \leq 3$ , an  $\{i, j\}$ -residue is also called an  $ij$ -gon or an  $i$ - and  $j$ -colored *bigon* (it is an even polygon, where the edges are alternatively colored  $i$  and  $j$ ). Denote by  $b(\mathcal{H})$  the total number of  $ij$ -gons for  $0 \leq i < j \leq 3$ . Denote by  $t(\mathcal{H})$  the total number of  $\bar{i}$ -residues for  $0 \leq i \leq 3$ , where  $\bar{i}$  means complement of  $\{i\}$  in  $\{0, 1, 2, 3\}$ .

We briefly recall the definition of gems taken from [9]. A 3-gem is a  $(3+1)$ -graph  $\mathcal{H}$  satisfying  $v(\mathcal{H}) + t(\mathcal{H}) = b(\mathcal{H})$ . This relation is equivalent to having the vertices, edges and bigons restricted to any  $\{i, j, k\}$ -residue inducing a plane graph where the faces are bounded by the bigons. Therefore we can embed each such  $\{i, j, k\}$ -residue into a sphere  $\mathbb{S}^2$ . We consider the ball bounded this  $\mathbb{S}^2$  as induced by the  $\{i, j, k\}$ -residue. For this reason an  $\{i, j, k\}$ -residue in a 3-gem,  $i < j < k$ , is also called a *triball*. An  $ij$ -gon appears once in the boundary of triball  $\{i, j, k\}$  and once in the boundary of triball  $\{i, j, h\}$ . By pasting the triballs along disks bounded by all the pairs of  $ij$ -gons,  $\{i, j\} \subset \{0, 1, 2, 3\}$  of a gem  $\mathcal{H}$ , we obtain a closed 3-manifold denoted by  $|\mathcal{H}|$ . This general con-

struction is dual to the one exemplified in the abstract and produces any closed 3-manifold. The manifold is orientable if and only if  $\mathcal{H}$  is bipartite, [7]. A *crystallization* is a gem which remains connected after deleting all the edges of any given color, that is, it has one  $\{i, j, k\}$ -residue for each trio of colors  $\{i, j, k\} \subset \{0, 1, 2, 3\}$ .

Let  $\mathcal{H}^*$  be the dual of a gem  $\mathcal{H}$ . An  $\bar{i}$ -residue of  $\mathcal{H}$  corresponds in  $\mathcal{H}^*$  to a 0-simplex of  $\mathcal{H}^*$ . Most 0-simplices of  $\mathcal{H}^*$  do not correspond to  $\bar{i}$ -residues of  $\mathcal{H}$ . An  $ij$ -gon of a gem  $\mathcal{H}$  corresponds in  $\mathcal{H}^*$  to a *PL1-face* formed by a sequence of 1-simplices of  $\mathcal{H}^*$ ; this PL1-face is the intersection of two PL2-faces of colors  $i$  and  $j$ ; their two bounding 0-simplices correspond to an  $\bar{h}$ - and to a  $\bar{k}$ -residue, where  $\{h, i, j, k\} = \{0, 1, 2, 3\}$ . An  $i$ -colored edge of  $\mathcal{H}$  corresponds to a *PL2-face* which is a 2-disk triangulated by a subset of  $i$ -colored 2-simplices of  $\mathcal{H}^*$ . Finally to a vertex of  $\mathcal{H}$ , it corresponds a *PL3-face* of  $\mathcal{H}^*$  which is a 3-ball formed by a subset of 3-simplices of  $\mathcal{H}^*$ .

**(1.1) Proposition.** *The 3-manifold induced by a  $J^2$ -gem  $\mathcal{H}$  is  $\mathbb{S}^3$ .*

**Proof.** Removing from  $\mathcal{H}$  all the edges of any given color produces a restricted graph which is connected (whose faces are bounded by the  $ij$ -gons). So  $\mathcal{H}$  has four 3-residues, one of each type. Denote by  $b_{ij}$  the number of  $ij$ -gons of  $\mathcal{H}$ . Each one of these residues are planar graphs having  $v = 2n$  vertices,  $3v/2$  edges and  $b_{12} + b_{13} + b_{23}$ ,  $b_{02} + b_{03} + b_{23}$ ,  $b_{01} + b_{13} + b_{03}$  and  $b_{12} + b_{01} + b_{02}$  faces for, respectively, the  $\bar{0}$ -,  $\bar{1}$ -,  $\bar{2}$ -,  $\bar{3}$ -residue. Adding the four formulas for the Euler characteristic of the sphere imply that  $v(\mathcal{H}) + 4 = b(\mathcal{H})$ . Therefore,  $\mathcal{H}$  is a crystallization having one  $0i$ -gon and one  $jk$ -gon. This implies that the fundamental group of the induced manifold is trivial: as proved in [6], the fundamental group of the space induced by a crystallization is generated by  $b_{0i} - 1$  generators, and in our case this number is 0. Since Poincaré Conjecture is now proved, we are done. However, we can avoid using this fact and, as a bonus, obtaining the validity of the next corollary, which is used in the sequel.

Assume that  $\mathcal{H}$  is a  $J^2$ -gem which does not induce  $\mathbb{S}^3$  and has the smallest possible number of vertices satisfying these assumptions. By planarity we must have a pair of edges of  $\mathcal{H}$  having the same ends  $\{p, q\}$ . Consider the graph  $\mathcal{H}fus\{p, q\}$  obtained from  $\mathcal{H}$  by removing the vertices  $p, q$  and the 2 edges linking them as well as welding the 2 pairs of pendant edges along edges of the same color. In [5] S. Lins proves that if  $\mathcal{H}$  is a gem,  $\mathcal{H}' = \mathcal{H}fus\{p, q\}$  is also a gem and that two exclusive relations hold regarding  $|\mathcal{H}|$  and  $|\mathcal{H}'|$ , their induced 3-manifolds: either  $|\mathcal{H}| = |\mathcal{H}'|$  in the case that  $\{p, q\}$  induces a 2-dipole or else  $|\mathcal{H}| = |\mathcal{H}'| \# (\mathbb{S}^2 \times \mathbb{S}^1)$ . Since  $\mathcal{H}'$  is a  $J^2$ -gem, by our minimality hypothesis on  $\mathcal{H}$  the valid alternative is the second. But this is a contradiction: the fundamental group of  $|\mathcal{H}|$  would not be trivial, because of the summand  $\mathbb{S}^2 \times \mathbb{S}^1$ .  $\square$

### 1.3 Dipoles, pillows and balloons

Suppose there are  $m$  edges linking vertices  $x$  and  $y$  of a gem,  $m \in \{1, 2, 3\}$ . We say that  $\{u, v\}$  is an  $m$ -*dipole* if removing all edges in the colors of the ones linking  $x$  to  $y$ , these vertices are in distinct components of the graph induced by the edges in the complementary set of colors. To *cancel the dipole* means deleting the subgraph induced by  $\{u, v\}$  and identify pairs of the hanging edges along the same remaining color. To *create the dipole* is the inverse operation. It is simple to prove that the manifold of a gem is invariant under dipole cancellation or creation. Even though is not relevant for the present work state the foundational result on gems: two 3-manifolds are homeomorphic if and only if any two gems inducing it are linked by a finite number of cancellations and creations of dipoles, [3, 8].

The dual of a 2-dipole  $\{u, v\}$ , with internal colors  $i, j$  is named a *pillow*. It consists of two PL3-faces  $\nabla_u$  and  $\nabla_v$  sharing two PL2-faces colored  $i$  and  $j$ . The *thickening of a 2-dipole into a 3-dipole* is defined as follows. Let  $i, j$  be the two colors internal to 2-dipole  $\{u, v\}$  and  $k$  a third color. Let  $a$  be the  $k$ -neighbor of  $x$  and  $b$  be the  $k$ -neighbor of  $y$ . Remove edges  $[a, x]$  and  $[b, y]$  and put back  $k$ -edges  $[u, v]$  and  $[r, s]$ . This completes the thickening. It is simple to prove that the thickening in a gem produces a gem. We must be careful because the inverse blind inverse operation *thinning a 3-dipole* not always produces a gem. The catch is that the result of the thinning perhaps is not a 2-dipole. In this sense the thinning move is not local: we must make sure that the result is a 2-dipole. To the data needed in thinning a 3-dipole  $\{u, v\}$  with internal colors  $\{i, j, k\}$  we must add the  $k$ -edge  $[r, s]$ . Note that the  $k$ -edges  $[u, v]$  and  $[r, s]$  are in the same  $hk$ -gon, where  $h$  is the fourth color. Denote by  $\Delta_{rs}$  the dual of  $[r, s]$ . Let  $\nabla_u \cup \nabla_v \cup \Delta_{rs}$  be called a *balloon*. Note that it consists of 2 PL3-faces  $\nabla_u$  and  $\nabla_v$  sharing three PL2-faces in colors  $\{i, j, k\}$  together with a  $k$ -colored PL2-face whose intersection with  $\nabla_u \cup \nabla_v$  is a PL1-face corresponding to the dual of the  $hk$ -gon, where  $h$  is the fourth color. Let  $\nabla_u \cup \nabla_v$  be the *balloon's head* and let  $\Delta_{rs}$  be the *balloon's tail*.

## 1.4 The Strategy for finding the $O(n^2)$ -algorithm

We want to find a PL-embedding for the dual  $\mathcal{H}^*$  of a  $J^2$ -gem  $\mathcal{H}$  into  $\mathbb{S}^3$ . To this end we remove one PL3-face of  $\mathcal{H}^*$  (one vertex of  $\mathcal{H}$ ) and find a PL-embedding in  $\mathbb{R}^3$  forming a PL-triangulated tetrahedron. After we use the inverse of a stereographic projection with center in the exterior of the triangulated tetrahedron. In this way we recover in  $\mathbb{S}^3$  the missing PL3-face.

In this work we describe the PL-embedded PL3-faces of  $\mathcal{H}^*$  into  $\mathbb{R}^3$  by making it geometrically clear that its boundary is a set of 4 PL2-faces, one of each color, forming an embedded  $\mathbb{S}^2$  whose interior is disjoint from the interior of  $\mathbb{S}^2$ 's corresponding to others PL3-faces. Thus, for our purposes it will be only necessary to embed the 2-skeleton of  $\mathcal{H}^*$ .

A direct approach to find the PL-embedding of the dual of a general  $J^2$ -gem with  $2n$  vertices, seems very hard. Therefore, we split the algorithm into 4 phases.

In the first phase we find a sequence of  $n - 1$  2-dipole thickenings into 3-dipoles not using color 3, where the new involved edge is either 0 or 1 so that the final gem is simply a circular arrangement of  $n$  3-dipoles with internal colors 0, 1, 2. Such a canonical  $n$ -gem is named a *bloboid* and is denoted  $\mathcal{B}_n$ . Such 3-dipoles are also named a *blob over a 3-colored edge*. A  $J^2\mathcal{B}$ -gem is a gem that, after canceling blobs over 3-colored edge becomes a  $J^2$ -gem. This indexing decreasing sequence is easily obtainable from the primal objects, in the case, simplifying  $J^2\mathcal{B}$ -gems until the bloboid is obtained:

$$\mathcal{H} = \mathcal{H}_n \xrightarrow[\text{thick}_1]{2\text{dip}} \mathcal{H}_{n-1} \xrightarrow[\text{thick}_2]{2\text{dip}} \dots \xrightarrow[\text{thick}_{n-1}]{2\text{dip}} \mathcal{H}_1 = \mathcal{B}_n = \mathcal{B}.$$

In the second phase we first find (phase 2A) specific abstract PL-triangulations, for the PL2-faces for the index increasing sequence of abstract colored 2-dimensional PL-complexes. Each of these complexes, latter, are going to be PL-embedded into  $\mathbb{R}^3$  so that the PL2-faces are topologically 2-spheres with disjoint interior. Attaching 3-balls bounded by these spheres we get the dual of the  $J^2$ -gem  $\mathcal{H}$  (with a vertex removed).

$$\mathcal{B}^* = \mathcal{H}_1^* \xrightarrow[\text{move}_1]{bp} \mathcal{H}_2^* \xrightarrow[\text{move}_2]{bp} \dots \xrightarrow[\text{move}_{n-1}]{bp} \mathcal{H}_n^* = \mathcal{H}^*.$$

In parallel to the construction of the sequence  $\mathcal{H}_m^*$ 's we also construct (phase 2B) a sequence of *wings*  $\mathcal{W}_m$ 's and their *nervures*  $\mathcal{N}_m$ 's so that  $\mathcal{S}_m = \mathcal{W}_m \cup \mathcal{N}_m$ , called a *strut*, is an adequate planar

graph, defined recursively. Moreover, wings and nervures are partitioned into their *left* and *right* parts:  $\mathcal{W}_m = \mathcal{W}'_m \cup \mathcal{W}''_m$  and  $\mathcal{N}_m = \mathcal{N}'_m \cup \mathcal{N}''_m$ . The sequence of struts is

$$\mathcal{S}_1^* = \mathcal{W}_1 \cup \mathcal{N}_1 \xrightarrow[\text{move}_1]{\text{wbp}} \mathcal{S}_2^* = \mathcal{W}_2 \cup \mathcal{N}_2 \xrightarrow[\text{move}_2]{\text{wbp}} \dots \xrightarrow[\text{move}_{n-1}]{\text{wbp}} \mathcal{S}_n^* = \mathcal{W}_n \cup \mathcal{N}_n = \mathcal{W} \cup \mathcal{N} = \mathcal{S}^*.$$

Each wing  $\mathcal{W}_m$ 's corresponds to a section of the previous sequence  $\mathcal{H}_m^*$ 's by two adequate fixed semi-planes  $\Pi'$  and  $\Pi''$ . The construction of the struts (which are planar graphs) is recursive. Initially  $\mathcal{W}_1^*$  is a set of  $2n$  lines incident to  $a_1$  and a set of  $2n$  lines incident to  $b_1$ , while  $\mathcal{N}_1^*$  is  $\emptyset$ . Going from  $\mathcal{S}_m^*$  to  $\mathcal{S}_{m+1}^*$  is very simple: two new vertices and four new edges appear, so as to maintain planarity.

In the third phase we make the abstract final element  $\mathcal{W}^* \cup \mathcal{N}^*$  of the second phase *rectilinearly* (that is each edge is a straight line segment) PL-embedded. By a cone construction we obtain from the rectilinearly PL-embedded strut  $\mathcal{S}^*$  a special PL-complex, named  $\mathcal{H}_1^\diamond$ . This complex does not correspond to a gem dual and it can be loosely explained as  $\mathcal{H}_1^*$  with all balloon's heads "opened".

The fourth phase, the *pillow filling phase* starts with  $\mathcal{H}_1^\diamond$  and the uses the abstract sequence  $\mathcal{H}_m^*$ 's to produce a pillow filling sequence

$$\mathcal{H}_1^\diamond \xrightarrow[\text{filling}_1]{\text{pillow}} \mathcal{H}_2^\diamond \xrightarrow[\text{filling}_2]{\text{pillow}} \dots \xrightarrow[\text{filling}_{n-1}]{\text{pillow}} \mathcal{H}_n^\diamond = \mathcal{H}^*.$$

In this phase everything is embedded into  $\mathbb{R}^3$  and the last element,  $\mathcal{H}^*$ , is the PL-embedding that we seek: the PL-embedding of the dual of the original  $J^2$ -gem  $\mathcal{H}$  minus a vertex into  $\mathbb{R}^3$ .

The whole procedure can be implemented as a formal algorithm that takes  $O(n^2)$ -space and  $O(n^2)$ -time complexity, where  $2n$  is the number of vertices of the original  $J^2$ -gem.

## 1.5 A complete example

In the example corresponding to Fig. 3, ..., Fig. 8 we gather and display the data structure we need for the  $O(n^2)$ -algorithm to PL-embed the dual of the  $J^2$ -gem  $\mathcal{H}_{12}$  of Fig. 8. The wings, nervures and their union, the struts, are partitioned into left and right parts:

$$\mathcal{W}_m = \mathcal{W}'_m \cup \mathcal{W}''_m, \quad \mathcal{N}_m = \mathcal{N}'_m \cup \mathcal{N}''_m, \quad \mathcal{S}_m^* = \mathcal{S}_m^{*'} \cup \mathcal{S}_m^{*''},$$

The sequence of figures displays the sequences of three data structures that we need: the inverse sequence of  $J^2B$ -gems  $\mathcal{H}_m$ , the colored 2-dimensional complexes  $\mathcal{H}_m^*$  (partitioned into colored PL2-faces) and the struts  $\mathcal{S}_m = \mathcal{W}_m \cup \mathcal{N}_m$ . The initial data structures are very simple and, in the figures we make clear how to obtain the next term of these sequences. In particular, the next colored 2-complex is given as the result of a *bp*-move, which changes a *balloon* into a *pillow*. See definitions in Subsection 2.2.3.

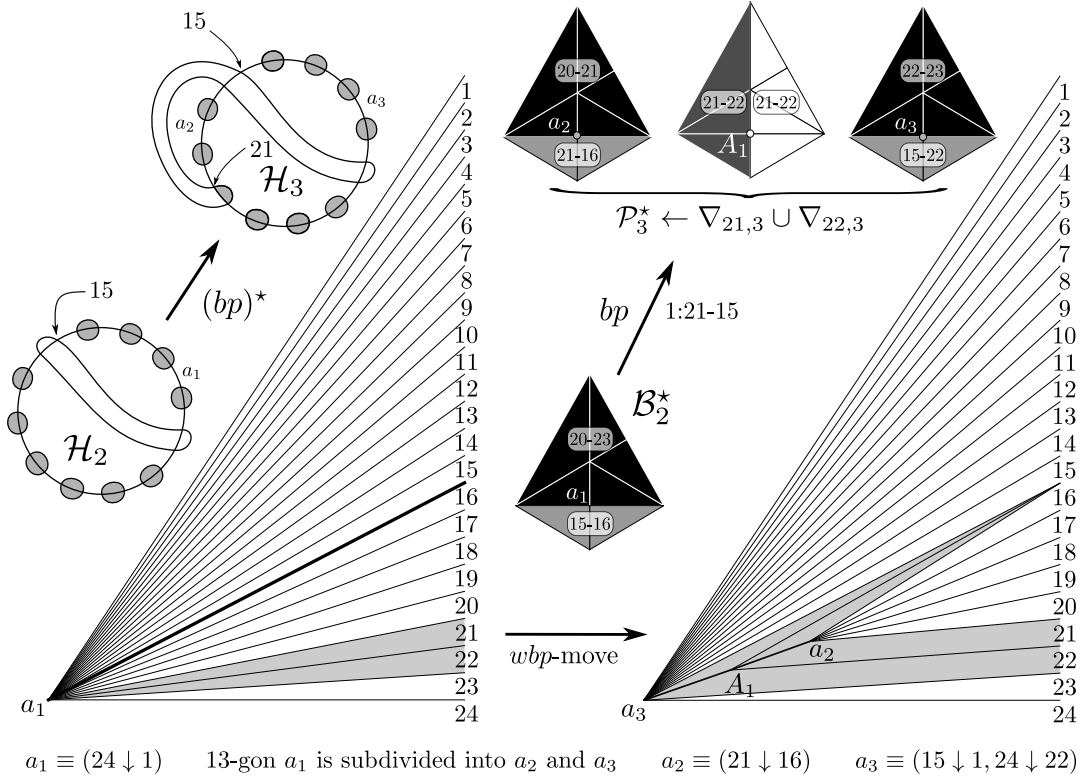
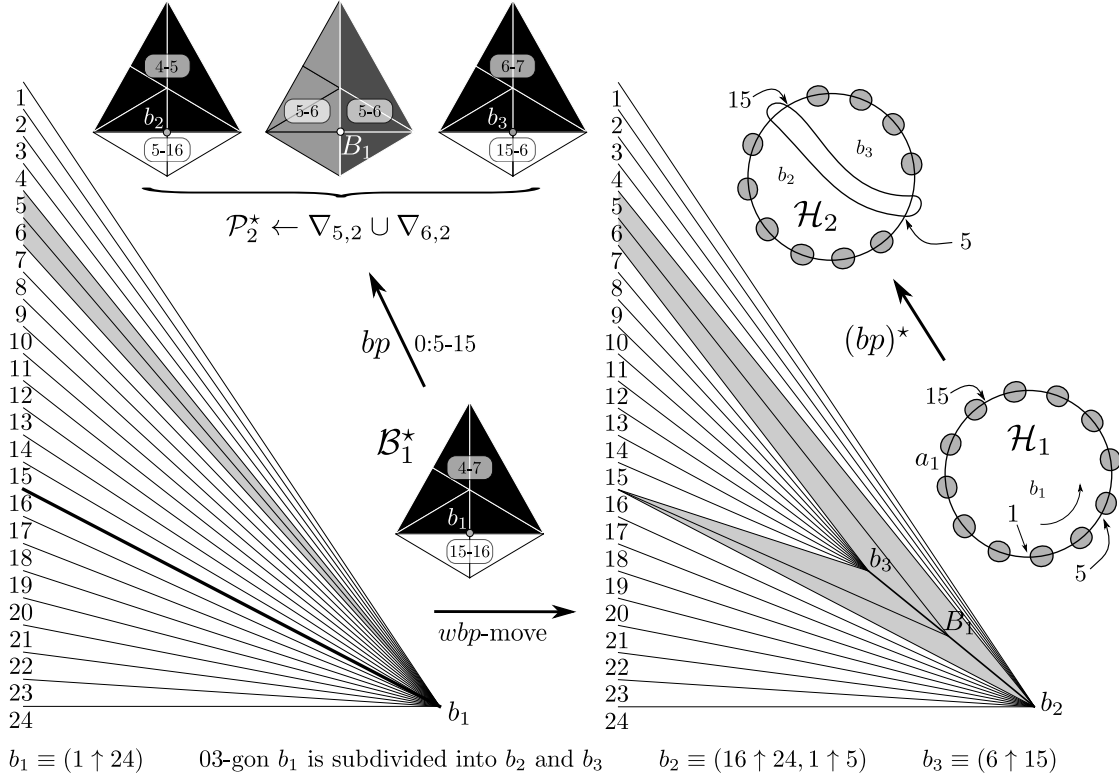


Figure 3: The initial right wing  $\mathcal{W}_1''$  is a set of lines emanating from  $b_1$ . The initial right nervure  $\mathcal{N}_1''$  is empty. The initial left wing  $\mathcal{W}_1'$  is a set of lines emanating from  $a_1$ . The initial left nervure  $\mathcal{N}_1'$  is empty. At the end of each  $wpb$ -move a pair of edges is added to the nervure. Lower case symbols  $a_j, b_k$  refer to 13-gons and 03-gons. Upper case symbols  $A_j, B_k$  are auxiliary 0-simplices.

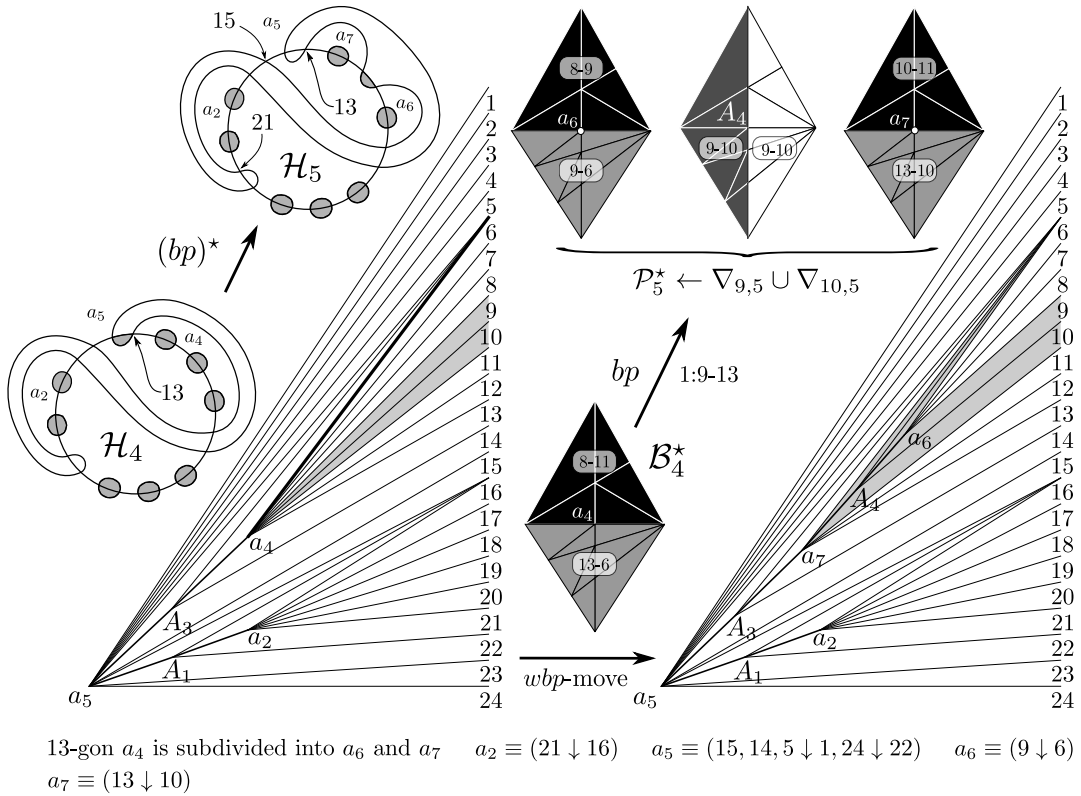
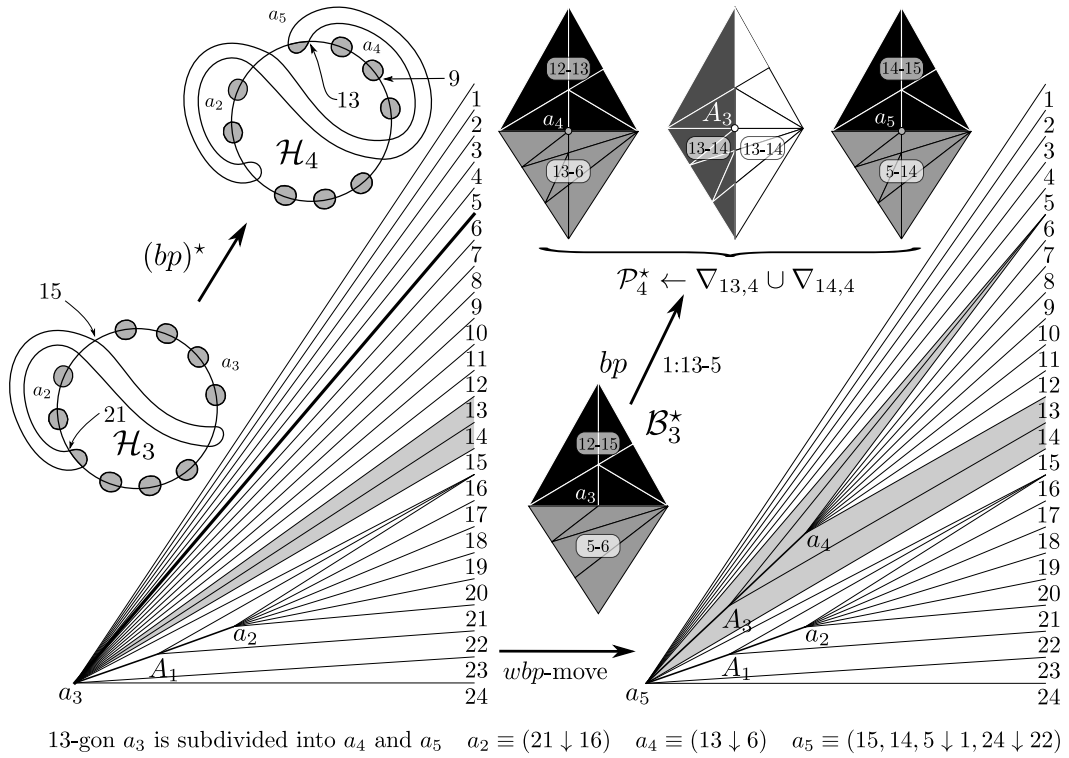
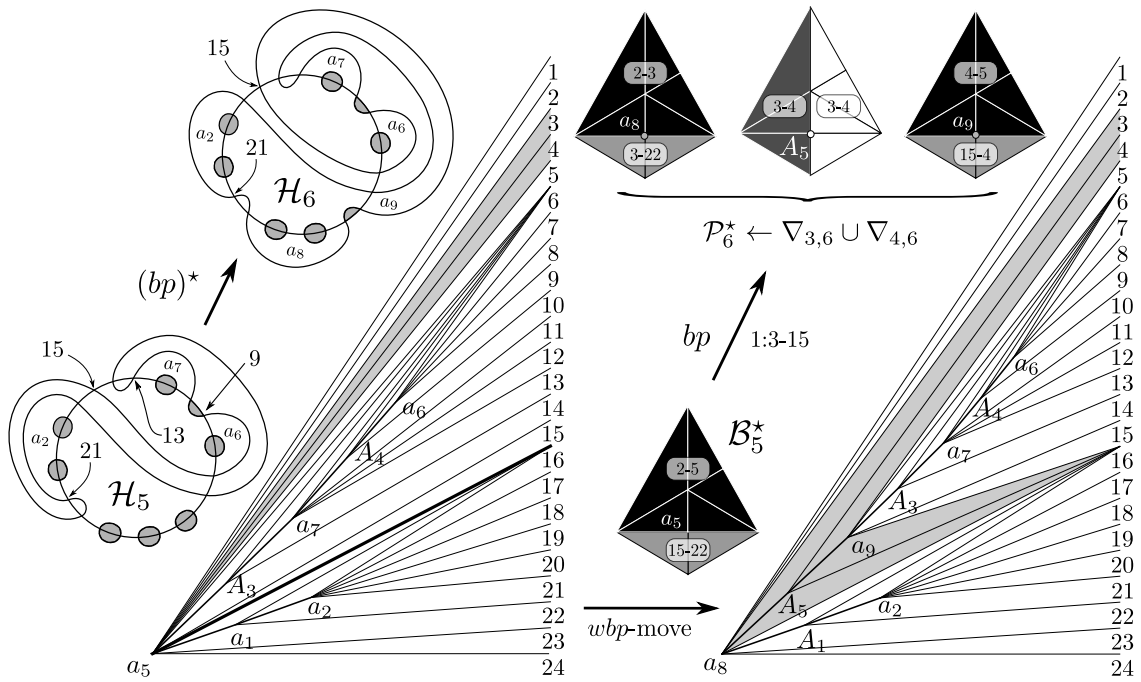
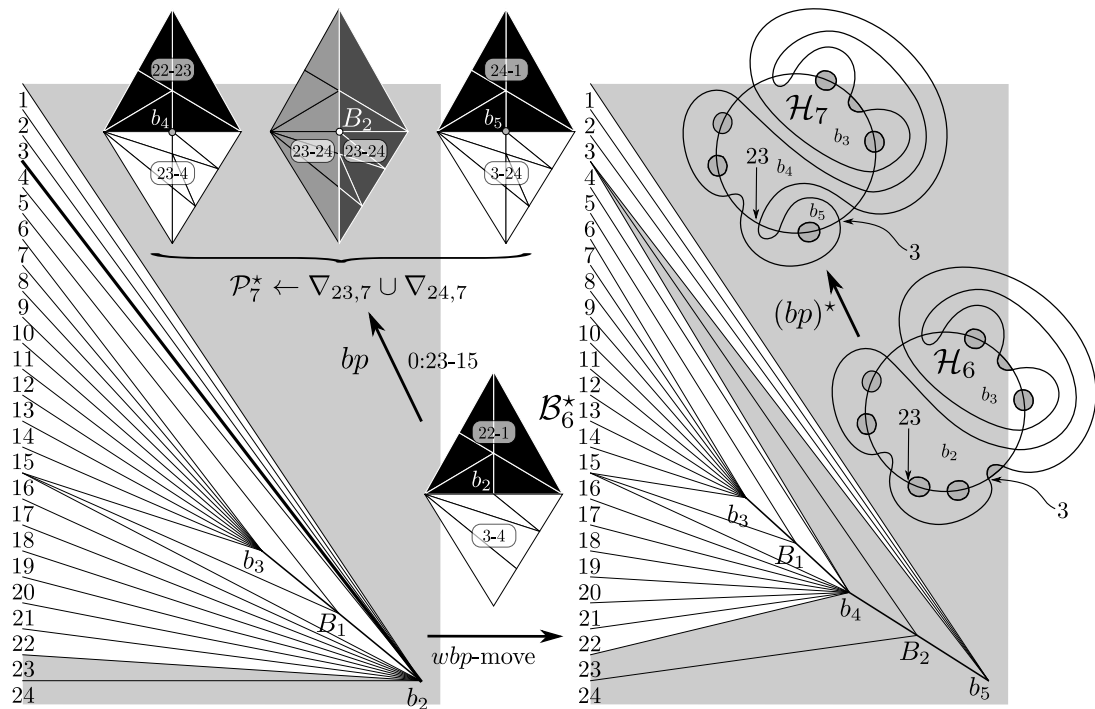


Figure 4: A left strut is modified by a *wbp*-move. What is needed as input is a pair of adjacent shaded triangles and a thick edge. In the lower left the strut is further modified by another *wbp*-move. The modification of balloons into pillows defines the new colored abstract combinatorial complexes. The nerves  $\mathcal{N}_m$  are auxiliary devices that will be disposed after we find the rectilinear embedded  $\mathcal{W}$  by a deterministic linear algorithm, See Fig. 8.



13-gon  $a_5$  is subdivided into  $a_8$  and  $a_9$   $a_2 \equiv (21 \downarrow 16)$   $a_6 \equiv (9 \downarrow 6)$   $a_7 \equiv (13 \downarrow 10)$   $a_8 \equiv (3 \downarrow 1, 24 \downarrow 22)$   
 $a_9 \equiv (15, 14, 5, 4)$



03-gon  $b_2$  is subdivided into  $b_4$  and  $b_5$   $b_3 \equiv (6 \uparrow 15)$   $b_4 \equiv (16 \uparrow 23, 4, 5)$   $b_5 \equiv (24, 1 \uparrow 3)$

Figure 5: In the first  $wbp$ -move a left strut is *extended based on*  $a_5$ . In all the figures of this  $r_5^{24}$ -example (except for the  $\mathcal{W}$  at the last one) we have used Tutte's barycentric method [17, 1] to obtain the embedded final struts. However, except for  $\mathcal{W}$ , only the combinatorics of the embeddings (the rotations) are needed to encode the struts in an implementation of the algorithm. In the second  $wbp$ -move one of the two shaded triangles is in the outside. Despite this special case, the rotation manifestation of the move behaves as usual.

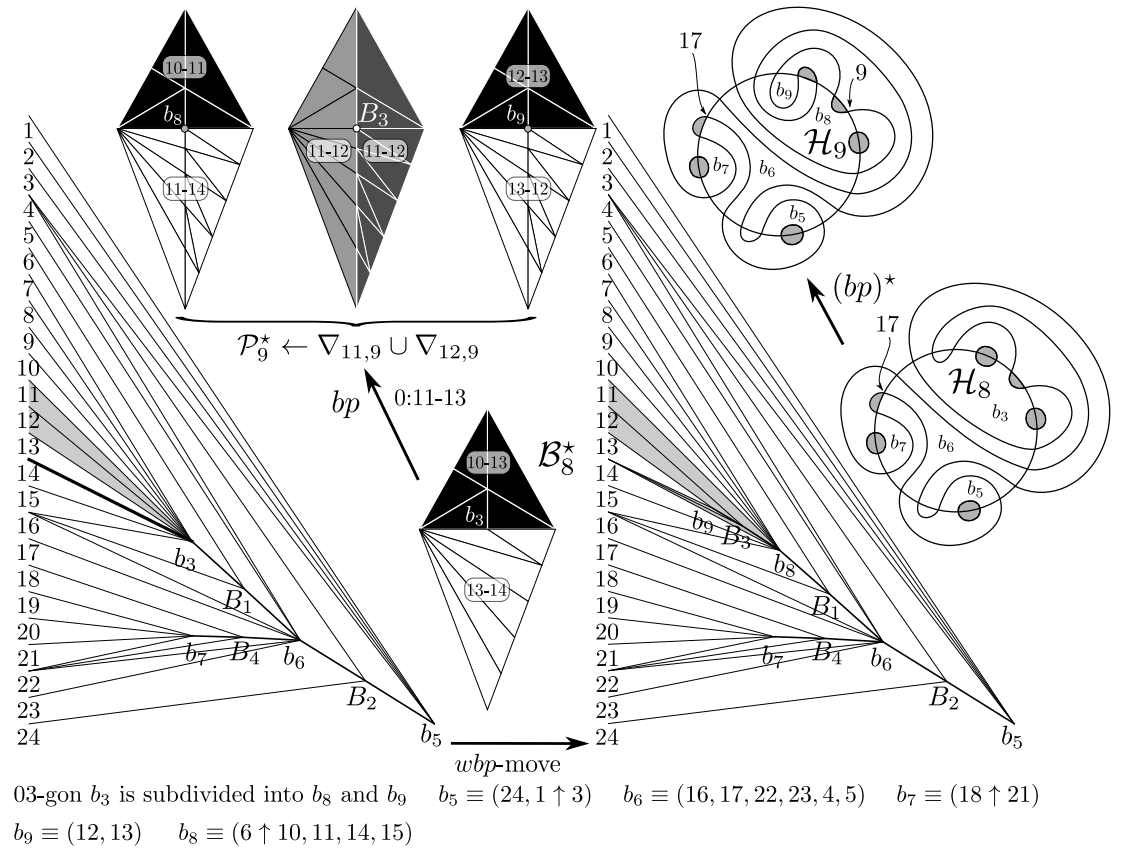
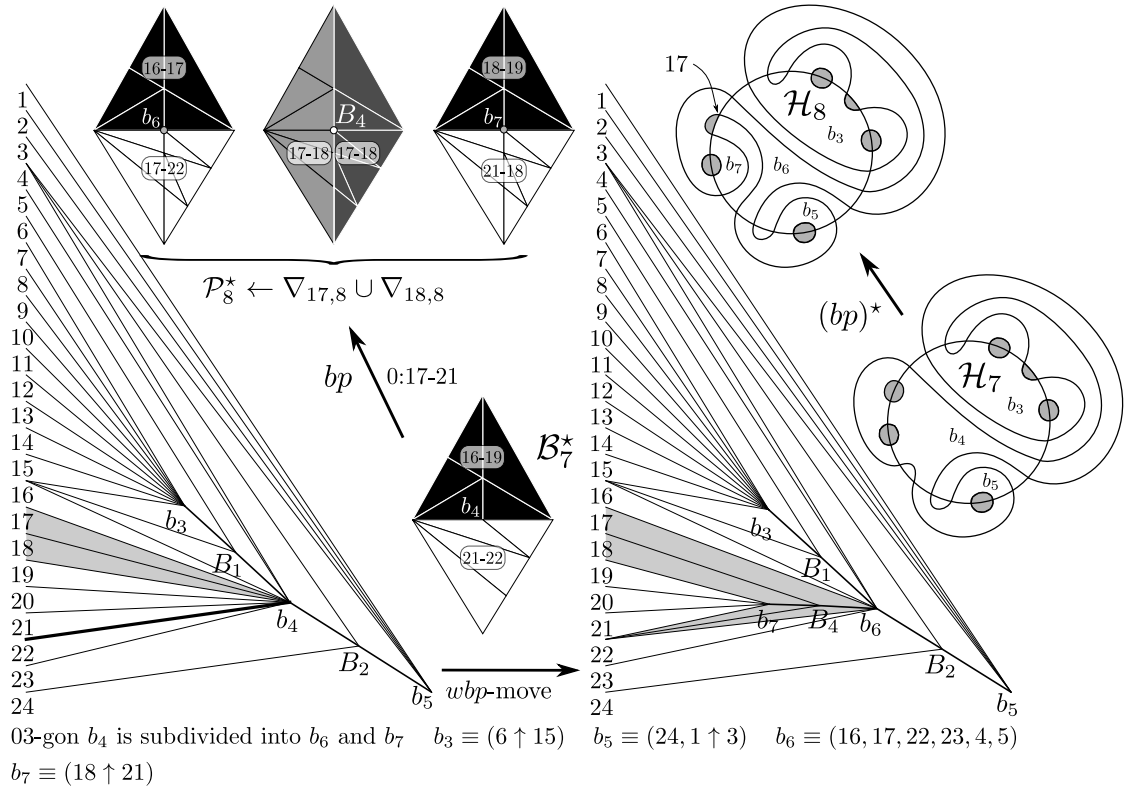


Figure 6: The first  $wbp$ -move induces a bifurcation on the nerve of a right wing based on  $b_4$ . The second  $wbp$ -move produces an extension based on  $b_3$  of the nerve of the final right wing of the first  $wbp$ -move.

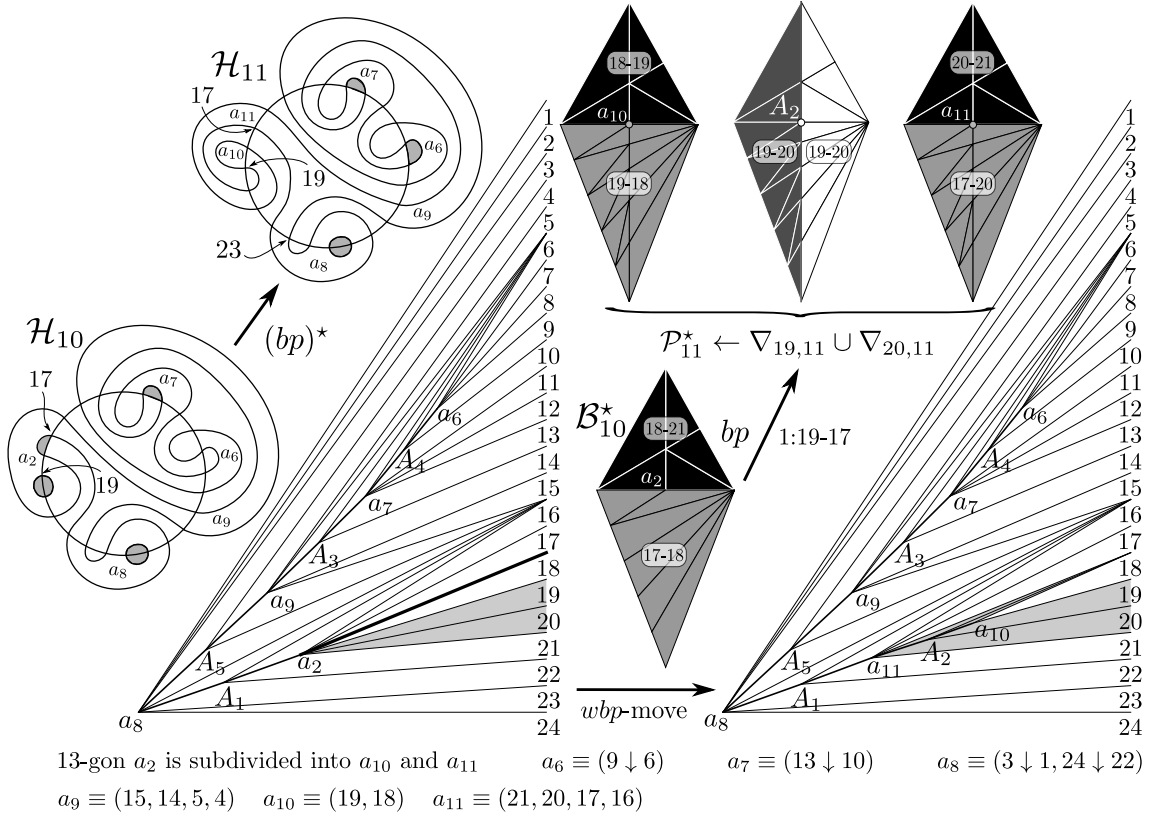
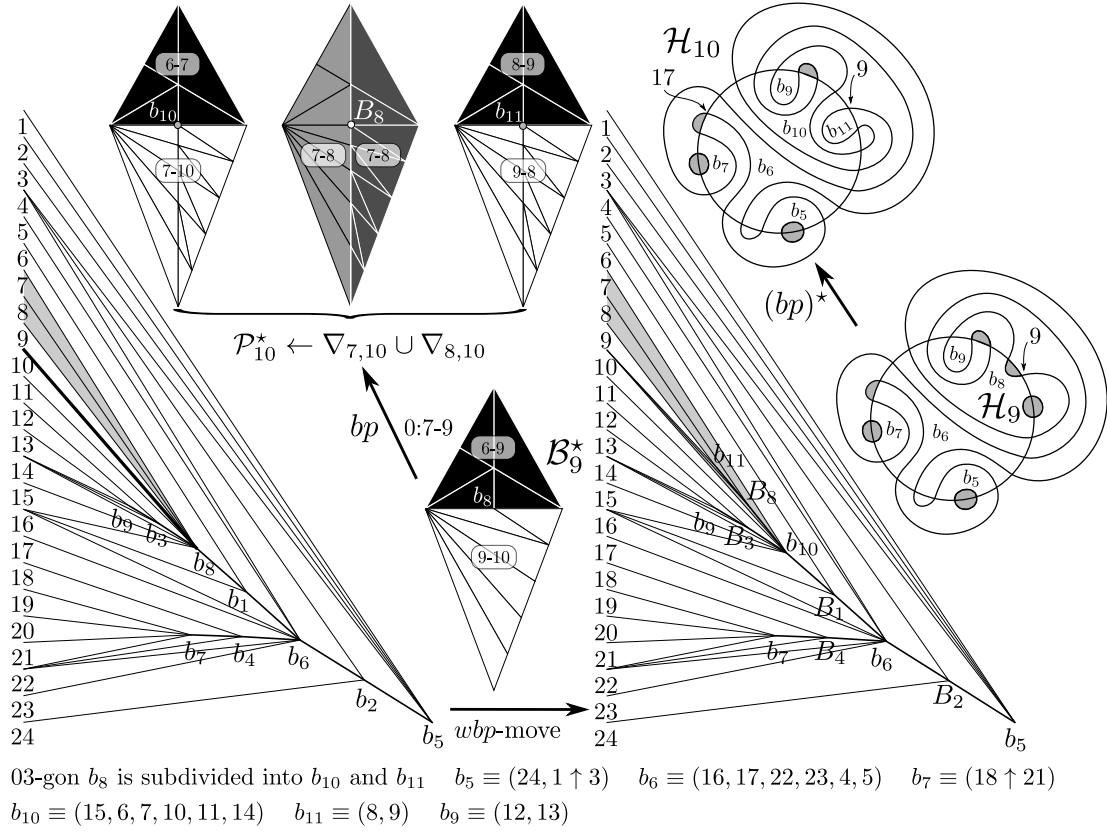


Figure 7: The first  $wbp$ -move induces another bifurcation on the nerve of a right wing based in  $b_8$ . The second  $wbp$ -move produces an extension of the nerve of a left wing based on  $a_2$ .

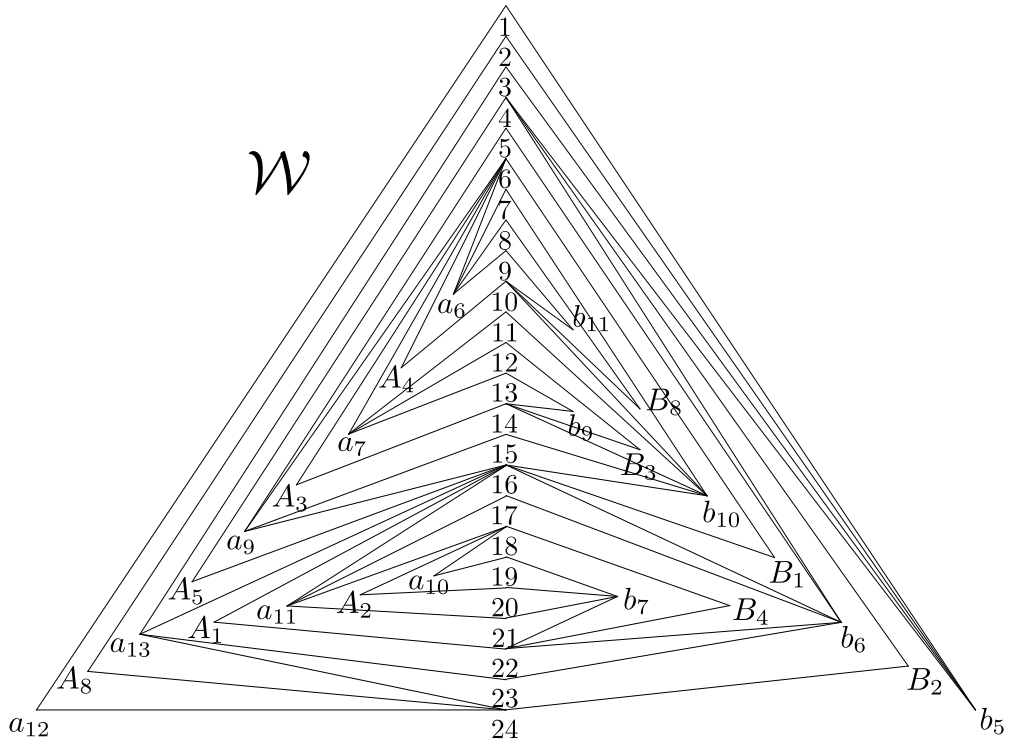
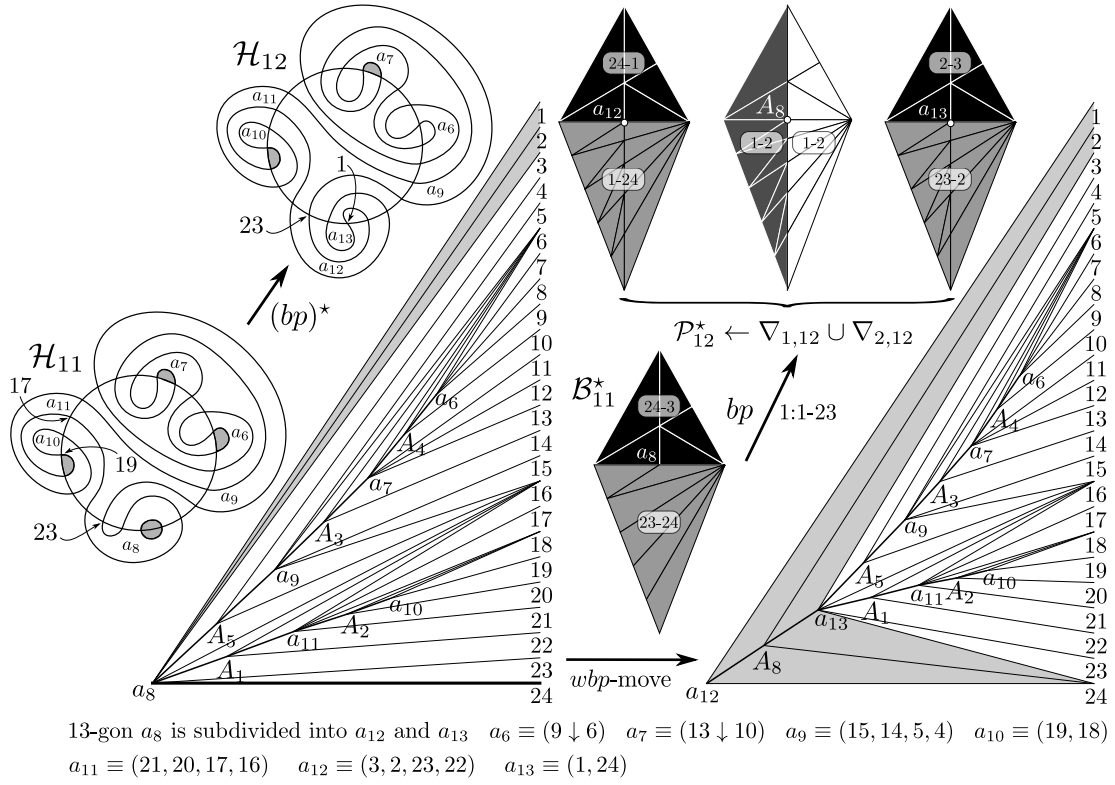


Figure 8: The globally last *wbp*-move is the extension based at  $a_8$  (corresponding to a 13-gon which breaks into two  $a_{12}$  and  $a_{13}$ ). The bottom part of the figure depicts the final pair of wings  $\mathcal{W}$ . This is the first time that the geometry of the embedding needs to be specified. Up to this point we need only the struts given combinatorially. To obtain the above embedding for  $\mathcal{W}$  we have used the deterministic linear algorithm explained in Subsection 2.3.

## 2 Details of the whole construction

### 2.1 First phase: from a $J^2$ -gem $\mathcal{H}$ to a bloboid $\mathcal{B}$

A  $k$ -dipole  $\{u, v\}$  involves color  $i$  if there is an edge of color  $i$  linking  $u$  to  $v$ .

Let  $H$  be the  $J^2$ -gem formed by the two Jordan curves  $X$  and  $Y$ . A  $(X, Y)$ -duet in  $H$  is a pair of crossings which are consecutive in  $X$  and in  $Y$ . A  $(X, Y)$ -trio in  $H$  is, likewise, a triple of crossings that are consecutive in  $X$  and in  $Y$ .

**(2.1) Lemma.** *Let  $H$  be a  $J^2$ -gem with  $2n \geq 4$  vertices. Then  $H$  has a  $(X, Y)$ -trio.*

**Proof.** By the Jordan theorem  $H$  has a  $(X, Y)$ -duet  $D$ . If  $n = 2$  then  $H$  has clearly a  $(X, Y)$ -trio establishing the basis of the induction. Suppose  $H$  has  $2n \geq 4$  vertices. It has a  $(X, Y)$ -duet  $D$ . If  $D$  extends to a trio, then we are done. Otherwise slightly deform  $Y$  to miss  $D$ . The resulting  $J^2$ -gem  $H'$  has  $2n - 2$  crossings and by induction hypothesis  $H'$  has a  $(X, Y)$ -trio  $T$ , which is present in  $H$ , establishing the Lemma.  $\square$

**(2.2) Proposition.** *Starting with a  $J^2$ -gem  $\mathcal{H}$  with  $2n$  vertices we can arrive to an  $n$ -bloboid  $\mathcal{B}$  by means of  $n - 1$  operations which thickens a 2-dipole involving color 2 into a 3-dipole, where the new edge is of color 0 or color 1, producing a sequence of  $J^2B$ -gems each inducing  $\mathbb{S}^3$ ,*

$$(\mathcal{H} = \mathcal{H}_n, \mathcal{H}_{n-1}, \dots, \mathcal{H}_2, \mathcal{H}_1 = \mathcal{B}).$$

**Proof.** The proof is by backward induction. For  $\ell = n$  we have  $\mathcal{H}_n = \mathcal{H}$  and so it is a  $J^2B$ -gem, establishing the basis of the induction. Assume that  $\mathcal{H}_\ell$  is a  $J^2B$ -gem. For  $\ell > 1$ , let  $\mathcal{H}'_\ell$  denote  $\mathcal{H}_\ell$  after canceling the blobs. By Lemma 2.1  $\mathcal{H}'_\ell$  has a  $(X, Y)$ -trio  $(x, y, z)$ . Thus  $y$  is incident to two 2-dipoles. One of these dipoles, call it  $D$ , involves color 2, the other involves color 3. Take the one involving color 2, name it  $D$ . Put back the blobs over the edges of color 3. So,  $D$  is present in  $\mathcal{H}_\ell$ . The colors involved in  $D$  are 0 and 2 or 1 and 2. In the first case we use color 1 to thicken  $D$  and in the second we use color 0 for the same purpose. This defines the  $J^2B$ -gem  $\mathcal{H}_{\ell-1}$ , which establishes the inductive step. In face of Proposition 1.1 and from the fact that thickening dipoles on gems produce gems inducing the same manifold, every member of the sequence induces  $\mathbb{S}^3$ .  $\square$

### 2.2 Second phase: colored abstract complexes, their wings, nervures

The second phase starts with an easy task, namely to define the dual of the bloboid, named  $\mathcal{H}_1^*$ . We get this first term in an embedded form. The others  $\mathcal{H}_2^*, \dots, \mathcal{H}_n^*$ , are, at this stage, obtained by slight modifications of the ancestor, but only in an abstract combinatorial way. In doing so we get the minimum level of refinement in the PL2-faces required, so that latter, the levels are sufficient for a geometric PL-embedding in  $\mathbb{R}^3$  which we seek.

#### 2.2.1 Primal and dual correspondence between the gem and the colored complex

There is a simple topological interpretation between primal and dual complexes, given in [9] pages 38, 39. Let us take a look at this interpretation in our context. This will help to understand the PL-embedding  $\mathcal{H}_m^*$ . In what follows the  $k$  in PL $k$ -face means the dimension  $k \in \{0, 1, 2, 3\}$  of the PL-face.

- i. a vertex  $v$  in  $G \iff$  a solid PL-tetrahedron or PL3-face, denoted by  $\nabla_v$  in the dual of the gem whose PL0-faces are labeled  $z_0, z_1, z_2 \in z_3^v$ ; in this work, it is enough to work with the boundary of a PL3-face; this is topologically a sphere  $\mathbb{S}^2$  with four PL2-faces one of each color; the 3-simplices forming a PL3-face need not be explicitly specified;
- ii. an  $i$  colored edge  $e_i$  in  $G \iff$  a set of  $i$ -colored 2-simplices defining a  $\text{PL}2_i$ -face in the dual of the gem;
- iii. a bigon  $B_{ij}$  using the colors  $i, j$  in  $G \iff$  a set of 1-simplices  $b_{ij}$  in  $\mathcal{H}_n^*$  defining a  $\text{PL}1_{ij}$ -face;
- iv. an  $\bar{i}$ -residue  $V_i$  in  $G \iff$  a 0-simplex in  $\mathcal{H}_n^*$  defining a  $\text{PL}0_i$ -face.

### 2.2.2 Defining $\mathcal{H}_1^*$ and the colored abstract PL-complexes: $\mathcal{H}_2^*, \dots, \mathcal{H}_n^*$

We define the combinatorial 2-dimensional PL complex  $\mathcal{H}_1^*$  as follows.

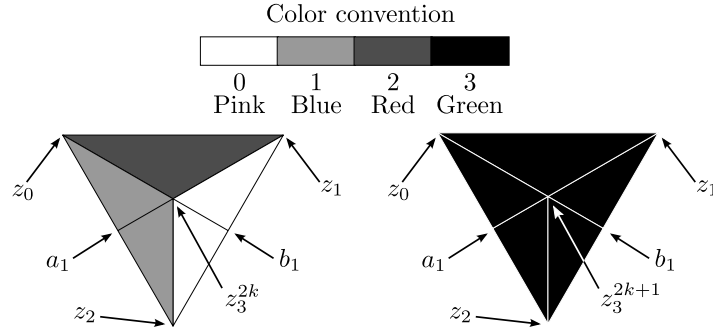


Figure 9: PL2-faces of  $\mathcal{H}_1^*$ : the figure is an abbreviation of a stack of tetrahedra, where  $k = 0, 1, \dots, n - 1$ . The 0-simplices  $z_3^j$  are defined as  $z_3^j = (0, 0, 2n - j)$ ,  $1 \leq j \leq 2n$ . For even  $j = 2k$ , there are five simplices incident to  $z_3^j$ : two 0-colored, two 1-colored and 1 2-colored. For odd  $j = 2k + 1$ , the five 2-simplices incident to  $z_3^j$  are all 3-colored. The 0-simplices  $z_0, z_1$  and  $z_2$  are positioned in clockwise order as the vertices of an equilateral triangle of side 1 in the  $xy$ -plane so that  $z_0z_1$  is parallel to the  $x$ -axis and the center of the triangle coincides with the origin of an  $\mathbb{R}^3$ -cartesian system. The 0-simplex  $a_1$  is  $\frac{z_0+z_2}{2}$ . The 0-simplex  $b_1$  is  $\frac{z_2+z_1}{2}$ . Note that, in general, the PL3-faces are given by their boundary. We never use 3-simplices explicitly to triangulate the PL3-faces. From our construction, however, it will be clear that this is possible to achieve without spurious intersections among the 3-simplices.

We detail the connection of the  $J^2$ -gem and its dual. In particular we use the unique 23-gons of it to provide labels  $1, 2, \dots, 2n$  in the cyclic order of the 23-gon. This labellings correspond to PL3-faces of the  $\mathcal{H}_1^*$  and will be maintained for the PL3-faces of the whole remaining sequence  $\mathcal{H}_2^*, \dots, \mathcal{H}_n^*$ . This invariance is a dual manifestation of the fact that in the thickening of dipoles the labels of the vertices preserved. Suppose  $u$  is an odd vertex of the  $J^2$ -gem,  $u' = u - 1$ ,  $v = u + 1$  and  $v' = v + 1$ . The dual of a  $\bar{3}$ -residue is  $z_3^j$  where  $j$  is even. When  $j$  is odd, then  $z_3^j$  is a 0-simplex in the middle of a  $\text{PL}2_3$ -face, incident to five 2-simplices of color 3. The dual of the 03-gon is the  $\text{PL}1$ -face formed by the pair of 1-simplices  $z_1b_1$  and  $b_1z_2$ . The dual of the 13-gon is the  $\text{PL}1$ -face formed by the pair of 1-simplices  $z_0a_1$  and  $a_1z_2$ . The dual of the 23-gon is the  $\text{PL}1$ -face formed by the 1-simplex  $z_0z_1$ . The dual of the 01-gon relative to vertices  $u$  and  $v$  is the 1-simplex  $z_2z_3^v$ .

The dual of the  $02$ -gon relative to vertices  $u$  and  $v$  is the 1-simplex  $z_1 z_3^v$ . The dual of the  $12$ -gon relative to vertices  $u$  and  $v$  is the 1-simplex  $z_0 z_3^v$ . The dual of a 3-colored edge  $u'v$  is the image of  $PL2_3$ -face with odd index  $u$  in the vertices. The dual of an  $i$ -colored edge  $uv$  with  $i \in \{0, 1, 2\}$  is the  $PL2_i$ -face with even index  $v$ .

### 2.2.3 Primal and dual $bp$ -moves

Before presenting  $\mathcal{H}_m^*$ ,  $1 < m \leq n$ , and its embeddings, we need to understand the dual of the  $(pb)^*$ -move and its inverse. In the primal, to apply a  $(pb)^*$ -move, we need a blob and a 0- or 1-colored edge. The dual of this pair is the *balloon*: the *balloon's head* is the dual of the blob; the *balloon's tail* is the dual of the  $i$ -edge. To make it easier to understand, the  $(pb)^*$ -move can be factorable into a 3-dipole move followed by a 2-dipole move, so in the dual, it is a smashing of the head of the balloon followed by the pillow move described in the book [9], page 39. This composite move is the *balloon-pillow move* or  $bp$ -move. Restricting our basic change in the colored 2-complex to  $bp$ -moves we have nice theoretical properties which are responsible for avoiding an exponential process.

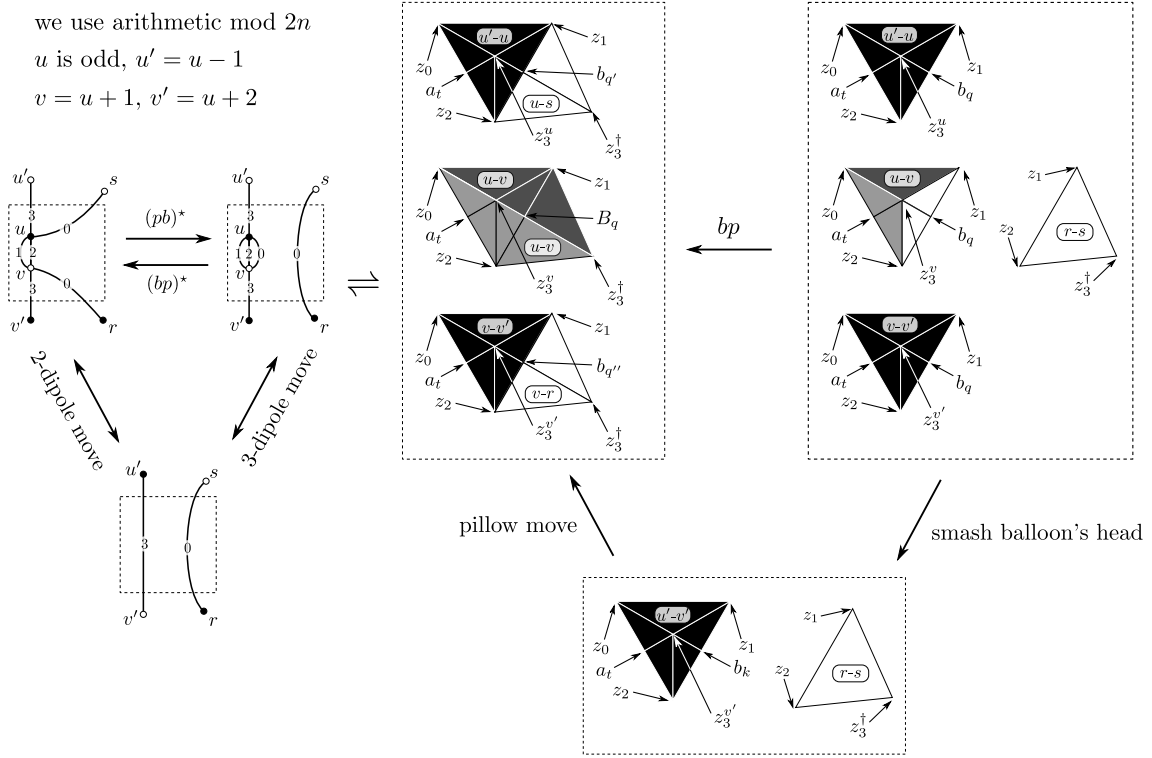


Figure 10: Primal and dual  $bp$ -moves: in what follows we describe the  $bp$ -move assuming that the balloon's tail is 0-colored using a generic balloon's tail, of which we just draw the contour. The other case, color 1, is similar. (1) if the image of  $v_5^u$  and  $v_5^v$  is  $b_q$ , create two 0-simplices  $b_{q'}$  and  $b_{q''}$ , define the images of  $v_5^u$  and  $v_5^v$  as  $b_{q'}$  and  $b_{q''}$  and change the label of the image of  $v_5^v$  from  $b_q$  to  $B_q$ ; (2) make two copies of the  $PL2_0$ -face, if necessary, refine each, from the middle vertex of the segment  $z_2 z_1$  to the third vertex  $z_3^\dagger$ , where  $\dagger = j$ , for an adequate height  $j$ ; (3) change the colors of the medial layer of the pillow as specified by the dual structure, namely by the current  $J^2 B$ -gem.

### 2.2.4 Types of PL2-faces

**(2.3) Proposition.** *Each PL2-face of the combinatorial simplicial complex  $\mathcal{H}_m^*$ ,  $1 \leq m \leq n$ , is isomorphic to one in the set of types of triangulations*

$$\{G, P_{2k-1}, P'_{2k-1}, B_{2k-1}, B'_{2k-1}, R_{2k-1}^b, R_{2k-1}^p \mid k \in \mathbb{N}\},$$

described in Fig. 11, where the index means the number of edges indicated and is called the rank of the type. Moreover, the PL2-faces that appear, as duals of the gem edges, have the minimum number of 2-simplices.

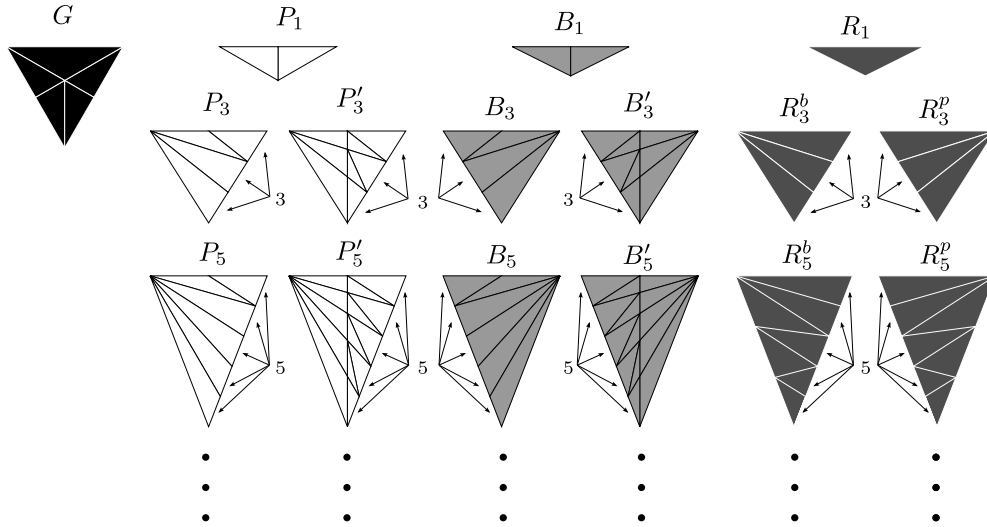


Figure 11: All kinds of PL2-faces that we use: the choice of the letters  $P, B, R, G$  comes from the colors  $0 = (P)ink$ ,  $1 = (B)lue$ ,  $2 = (R)ed$  and  $3 = (G)reen$ . Define  $R_{2k-1}^b$  as the PL2<sub>2</sub>-face which is inside the pillow neighboring a PL2<sub>1</sub>-face. Similarly  $R_{2k-1}^p$  is a PL2<sub>2</sub>-face which is inside the pillow neighboring a PL2<sub>0</sub>-face. These PL2-faces are for now abstract combinatorial triangulations that have the correct level of refinement so as to become PL-embedded into  $\mathbb{R}^3$ .

**Proof.** We need to fix a notation for the head of the balloon. Instead of drawing all the PL2-faces of the head, we just draw one PL2<sub>3</sub>-face and put a label  $u'-v'$ . If the balloon's tail, is of type  $P_1$ , by applying a  $bp$ -move we can see at Fig. 12 that we get a PL2<sub>1</sub>-face of type  $B_3$  and a

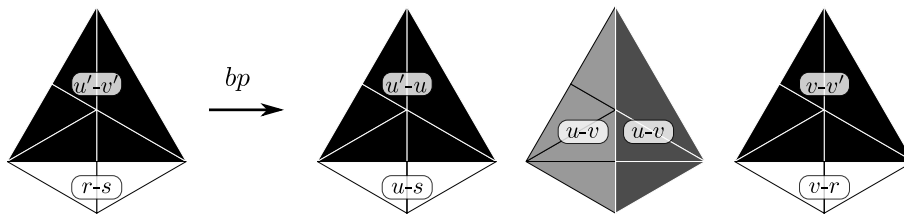


Figure 12: A  $bp$ -move with the balloon's tail of type  $P_1$ .

PL2<sub>2</sub>-face of type  $R_3^b$ . The others PL2-faces are already known. If the balloon's tail, is of type

$B_3$ , by applying a  $bp$ -move, we need to refine the tail and the copies, otherwise we would not be able to build a pillow because some 2-simplices would be collapsed, so we get two  $PL2_1$ -faces of type  $B'_3$ , one  $PL2_0$ -face of type  $P_5$  and a  $PL2_2$ -face  $R_5^p$ . The others  $PL2$ -faces are already known.

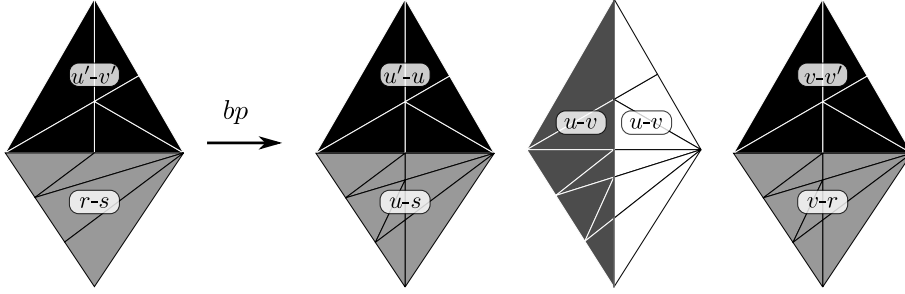


Figure 13: A  $bp$ -move with the balloon's tail of type  $B_3$ .

In what follows given  $X \in \{P'_{2k-1}, B'_{2k-1}\}$  denote by  $\overline{X}$  the copy of  $X$  which is a  $PL2$ -face of the  $PL$ -tetrahedra whose  $PL2_3$ -face is below the similar  $PL2_3$ -face of the other  $PL$ -tetrahedra which completes the pillow in focus. In face of these conventions, if balloon's tail is of type

- $P_{2k-1}$ , then by applying a  $bp$ -move, we get types  $P'_{2k-1}, \widehat{P}'_{2k-1}, B_{2k+1}, R_{2k-1}^b$
- $P'_{2k-1}$ , then by applying a  $bp$ -move, we get types  $P_{2k-1}, B_{2k+1}, R_{2k-1}^b$
- $B_{2k-1}$ , then by applying a  $bp$ -move, we get types  $B'_{2k-1}, \widehat{B}'_{2k-1}, P_{2k+1}, R_{2k-1}^p$
- $B'_{2k-1}$ , then by applying a  $bp$ -move, we get types  $B_{2k-1}, P_{2k+1}, R_{2k-1}^p$

The necessary increasing in the ranks of the types of faces shows that the rank of each face is at least the one obtained. It may cause a surprise the fact that these ranks are enough to make the  $PL$ -embedding geometric into  $\mathbb{R}^3$ .  $\square$

It is worthwhile to mention, in view of the above proof, that each  $PL2$ -face is refined at most one time. So, if  $X$  is a type of  $PL2$ -face,  $X'$  is its refinement, then  $X'' = X'$ . This idempotency is a crucial property inhibiting the exponentiality of our algorithm and enables a quadratic bound.

## 2.2.5 Quadratic bounds on the number of simplices

(2.4) **Corollary.** *The quadratic expressions*

$$3n^2 - 5n + 9, \quad 11n^2 - 17n + 21, \quad 8n^2 - 10n + 12$$

are upper bounds for the numbers of 0-simplices, 1-simplices and 2-simplices of the colored 2-complex  $\mathcal{H}_n^*$  induced by a resolvable gem  $G$  with  $2n$  vertices.

**Proof.** We prove the first bound, on 0-simplices; the other are similar: in the worse case, the increase of simplices is a linear function on the rank of the current  $PL2$ -face, and to get the final number we sum an arithmetic progression.

We detail the strategy for 0-simplexes. Note that  $\mathcal{H}_1^*$  has exactly  $z_0, z_1, z_2, a_1, b_1$  and  $z_3^j, j \in \{1, \dots, 2n\}$  as 0-simplices, which is  $2n + 5$  0-simplices. In the first step, the balloon's tail has

to be of type  $P_1$  or  $B_1$ , so by applying a  $bp$ -move, we get two new 0-simplices. In second step, the worst case is when the balloon's tail is of type  $P_3$  or  $B_3$ , generated by last  $bp$ -move, so we add  $6 \times 1 + 2 = 8$  to the number of 0-simplices in the upper bound. In step  $k$  we note that the worst case is when we use the greatest ranked PL2-face generated by last  $bp$ -move, therefore the balloon's tail has to be of type  $P_{2k-1}$  or  $B_{2k-1}$  and we add  $6 \cdot (k - 1) + 2$  0-simplices. By adding the number of 0-simplices created by  $bp$ -moves from step 1 until step  $k$  we get  $3k^2 - k$  0-simplices. Since the number of steps is  $n - 1$ , and we have at the beginning  $2n + 5$  0-simplices, we have that  $3n^2 - 5n + 9$  is an upper bound for the number of 0-simplices.  $\square$

### 2.2.6 Detailing the combinatorics of the wings, nervures and struts

An embedding of a graph into an oriented surface is combinatorially encoded as a *rotation at the vertices* or simply a *rotation*. A rotation is the set of cyclic orderings of the edges around the vertices (induced by the surface) so that each edge appears exactly twice, one with each orientation. We encode the struts as rotations. Only the last one needs to be dealt with geometrically.

At some point in our research it became evident that what was needed to obtain the embedded PL-complex  $\mathcal{H}_n^*$  was a proper embedding into  $\mathbb{R}^3$  of two special sequences of 0-simplices  $\mathcal{A} = (a'_1, a'_2, \dots, a'_f)$  and  $\mathcal{B} = (b'_1, b'_2, \dots, b'_g)$ , where  $f + g = 2n$ . Each  $a'_i \in \{a_i, A_i\}$  and each  $b'_i \in \{b_i, B_i\}$ . This terminology for the 0-simplices is obtained recursively and detailed shortly in this section. For now we just say that all other 0-simplices not in  $\mathcal{A} \cup \mathcal{B}$  of the colored complexes  $\mathcal{H}_m^*$  are obtained by bisections of segments linking previously defined points. It came as a surprise to discover that the apparently difficult 3D problem of positioning  $\mathcal{A} \cup \mathcal{B}$  could be reformulated as a plane problem with an easy solution, via a linear unique solution algorithm. That is the role of the wings, nervures and struts associated to the colored complexes.

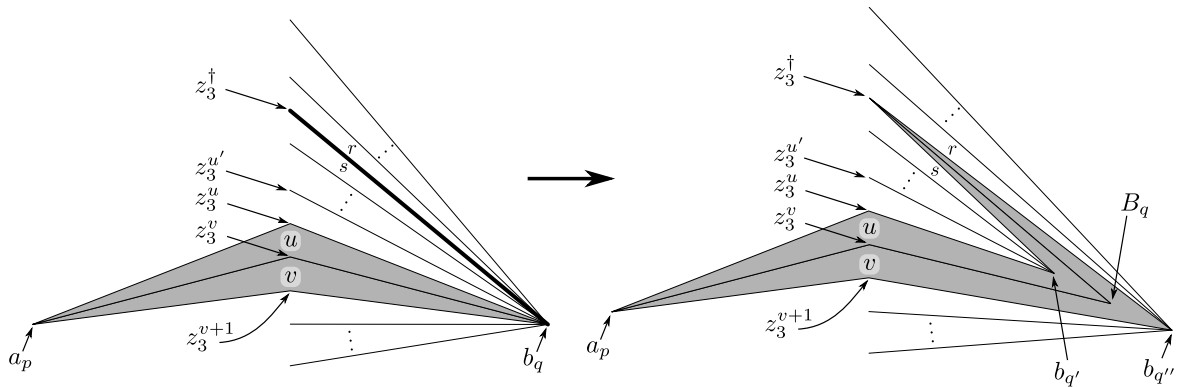


Figure 14: Generic  $wbp$ -move: balloon's head section is painted in gray, and the part of balloon's tail that is intersecting the appropriate semi-plane ( $\Pi''$ ) is depicted as a *thick edge*.

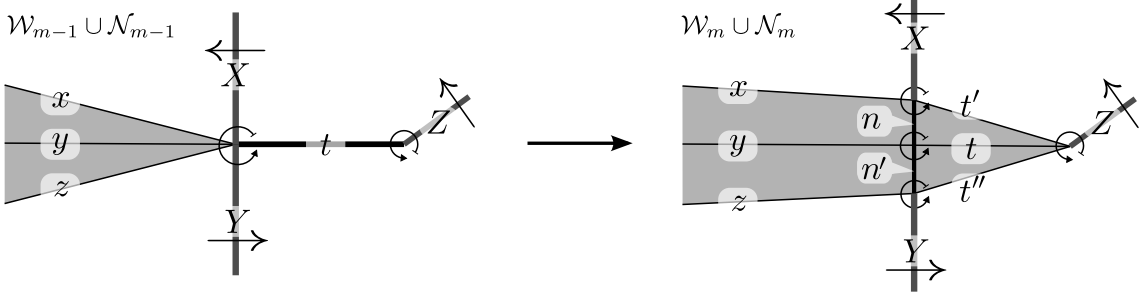


Figure 15: The effect of the general *wbp*-move in the combinatorial strut: the *star* of a vertex of a graph embedded in an orientable surface (in our case the plane) is the counterclockwise cyclic sequence of edges incident to the vertex (such an ordering is induced by the surface). The set of stars is called a *rotation* and has the characterizing property that each edge appears twice. The general case of changing rotation when going from  $\mathcal{W}_{m-1} \cup \mathcal{N}_{m-1}$  to  $\mathcal{W}_m \cup \mathcal{N}_m$  is depicted above: labels  $X, Y, Z$  stand for arbitrary (maybe empty) sequences of edges; the vertex  $XxyzYt$  breaks into three  $Xxnt'$ ,  $nyn't$  and  $n'zYt''$  and the vertex  $Zt$  changes into  $Zt't''$ . Two new vertices and four new edges are created. Two of these edges ( $n$  and  $n'$ ) are in the nervure  $\mathcal{N}_m$  and the other two ( $t'$  and  $t''$ ) are in the wing  $\mathcal{W}_m$ . The new rotation completely specifies the topological embedding of  $\mathcal{W}_m \cup \mathcal{N}_m$ .

**(2.5) Algorithm (Obtaining the rotations for the struts, arriving to  $\mathcal{S}_n$ ).** BEGIN:  $i = 1$ ;  $\mathcal{W}_i = \mathcal{W}'_i \cup \mathcal{W}''_i$  is formed by  $2n$ -edges linking  $a_1$  to  $Z$  and  $2n$  edges linking  $b_1$  to  $Z$ ; we also have  $\mathcal{N}_1 = \emptyset$ ; REPEAT:  $i \leftarrow i + 1$ ; there are two cases, according to the color of the edges which are flipped in the associated thinning of a blob is 1 or 0; in the first case the strut that changes is the left one (while  $\mathcal{S}''_i = \mathcal{S}''_{i-1}$ ), in the other case it is the right strut that changes (while  $\mathcal{S}'_i = \mathcal{S}'_{i-1}$ ); perform the appropriate *wbp*-move creating two new vertices  $a_{2\ell}, a_{2\ell+1}$  in the first case or  $b_{2\ell}, b_{2\ell+1}$  in the second ( $2\ell - 1$  is the last index of  $\mathcal{A}$  or of  $\mathcal{B}$ ); let  $a_q$  (resp.  $b_q$ ) denote the 13-gon (resp. the 03-gon) which is being subdivided; then we relabel  $a_q$  as  $A_q$  (resp.  $b_q$  as  $B_q$ ); these capital letter labeled 0-simplices no longer correspond to bigons, while bigon  $a_q$  (resp  $b_q$ ) has been subdivided into  $a_{2\ell}, a_{2\ell+1}$  (resp.  $b_{2\ell}, b_{2\ell+1}$ ); also 2 new edges are added when going from  $\mathcal{S}_{m-1}$  to  $\mathcal{S}_m$  according to the rotation changing of Fig. 15; UNTIL  $i = n$ ; Output  $\mathcal{S}_n$ ; END.

It is easy to verify that the above algorithm is linear in  $n$ . Now we need to make  $\mathcal{S}'_n$  rectilinearly embedded into  $\Pi'$  and  $\mathcal{S}''_n$  rectilinearly embedded into  $\Pi''$ . This is provided in the next subsection.

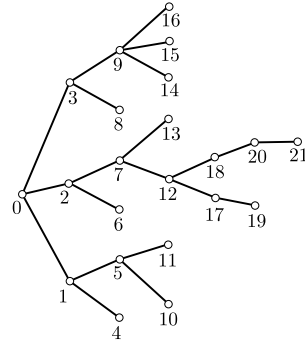
### 2.3 Third phase: a rectilinear PL-embedding for $\mathcal{S}_n$ and its induced diamond complex $\mathcal{H}_1^\diamond$ , by a cone construction

A graph is *rectilinearly embedded into a plane* if the images of their edges are straight line segments. We will find by a linear algorithm a rectilinear embedding for  $\mathcal{S}_n$ . We do it in the plane and lift it to space by two simple rotations to position  $\mathcal{S}'_n$  in  $\Pi'$  and  $\mathcal{S}''_n$  in  $\Pi''$ .

**(2.6) Lemma.** *The number of edges of  $\mathcal{S}_n$  is  $8n - 4$ .*

**Proof.** The number of edges of  $\mathcal{S}_1$  is  $4n$ . At each of the  $n - 1$  *bp*-moves we add 4 new edges.  $\square$

We present an algorithm to obtain a rectilinear embedding in the plane  $xz$  of  $\mathcal{S}_n$ . The algorithm is subdivided into two sub-algorithms: the first one produces the  $x$ -coordinates of the vertices of  $\mathcal{N}_n$  and the second one produce the  $z$ -coordinates of the vertices of  $\mathcal{S}_n$ .



- $\pi_1 : 21-20-18-12-7-2-0$
- $\pi_2 : 19-17-12$
- $\pi_3 : 16-9-3-0$
- $\pi_4 : 15-9$
- $\pi_5 : 14-9$
- $\pi_6 : 13-7$
- $\pi_7 : 11-5-1-0$
- $\pi_8 : 10-5$
- $\pi_9 : 8-3$
- $\pi_{10} : 6-2$
- $\pi_{11} : 4-1$

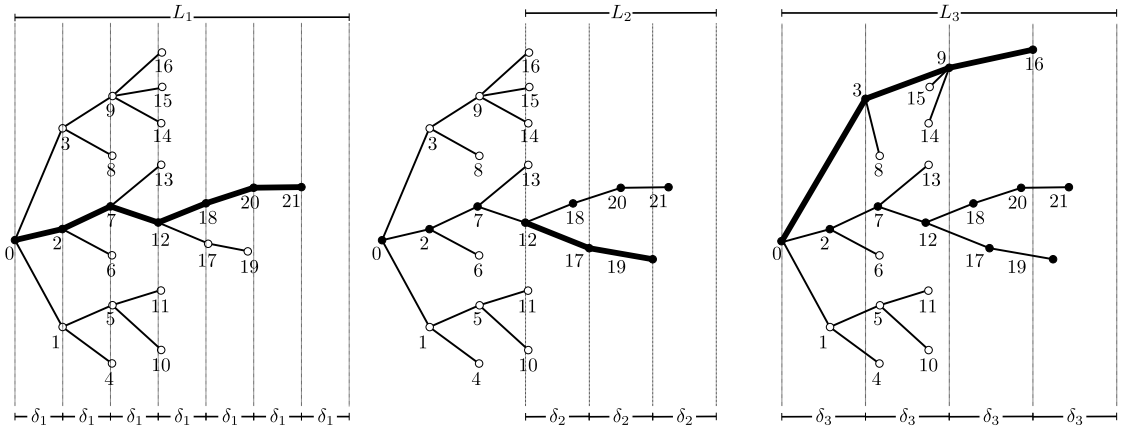


Figure 16: A linear sub-algorithm to find the  $x$ -coordinates of the vertices of the left nervure  $\mathcal{N}'$  (the right nervure  $\mathcal{N}''$  is similar). BEGIN: find the BFS-number ([2]) of vertices of the tree  $\mathcal{N}'$  with root vertex being the leftmost one of  $\mathcal{N}'$ . Let the vertices be labeled by its BFS-number. In the algorithm, we use a partition of the edges of  $\mathcal{N}'$  into paths; make all vertices except the root unused;  $i = 0$ ; make the path partition empty; REPEAT:  $i \leftarrow i + 1$ ; take the ancestor path  $\pi_i$  starting with the highest BFS-numbered vertex not yet used and finishing at the first used vertex; put the sequence of vertices of  $\pi_i$  defining a new member of the edge-path partition; declare all the vertices in  $\pi_i$  as used; let  $\delta_i$  be  $L_i/\lambda_i$ , where  $L_i$  is the  $x$ -distance from the first and last vertices of  $\pi_i$  and  $\lambda_i$  is the number of vertices in  $\pi_i$ ; let  $\delta_i$  be the  $x$ -distance between consecutive vertices of  $\pi_i$  (note that the  $x$ -coordinate of the last vertex of  $\pi_i$  has been already defined and so the  $x$ -coordinates of the all the vertices of  $\pi_i$  becomes fixed, never to change); UNTIL all vertices are used; END.

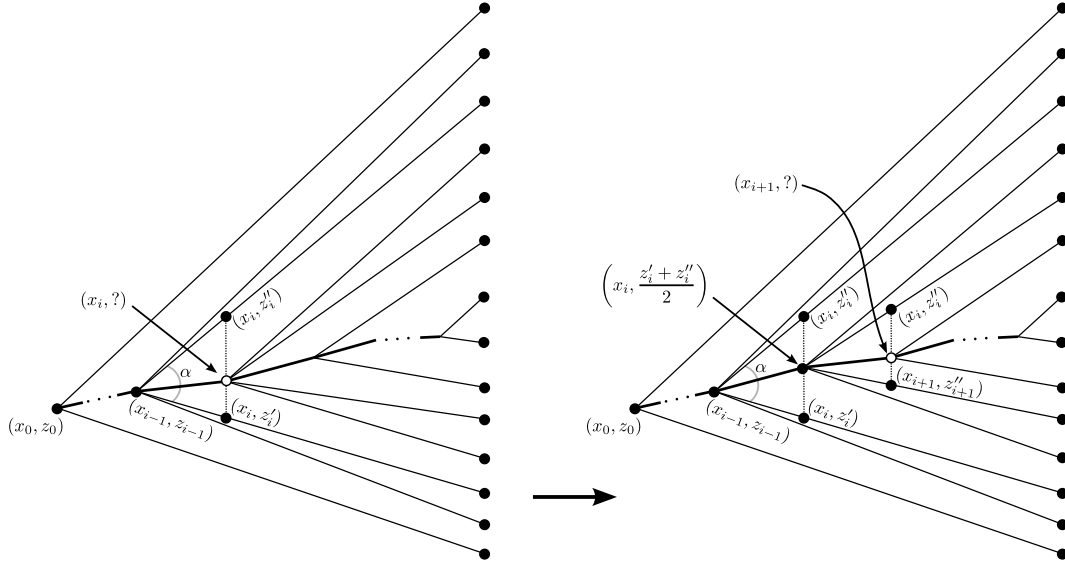


Figure 17: A linear sub-algorithm to find the  $z$ -coordinates of the vertices for a rectilinear embedding of  $\mathcal{W}'$  ( $\mathcal{W}''$  is similar). BEGIN: by using the Algorithm of Fig. 16 we have already the  $x$ -coordinates of all the vertices of  $\mathcal{W}'$ . Let  $\gamma_1, \gamma_2, \dots, \gamma_k$  be the sequence of inverses of the paths  $\pi_i$ 's, obtained in the algorithm of Fig. 16; let  $z_1^1$  be the  $z$ -coordinate of the first vertex of  $\gamma_1$ ;  $z_1^1 \leftarrow 0$ ;  $i \leftarrow 0$ ; REPEAT:  $i \leftarrow i + 1$ ;  $j \leftarrow 0$ ; REPEAT:  $j \leftarrow j + 1$ ; let  $e_{ij}$  be the edge in the nervure incident to  $\gamma_i^j$  (the  $j$ -th vertex in the path  $\gamma_i$ ) and  $\gamma_i^{j-1}$ ; let  $e'_{ij}$  be the edge which succeeds  $e_{ij}$  and  $e''_{ij}$  be the edge that precedes it in the counterclockwise rotation of vertex  $\gamma_i^{j-1}$ ; note that the other ends of  $e'_{ij}$  and  $e''_{ij}$  are  $z_3^p$  and  $z_3^q$  for some  $p < q$ ; (Obs: in the case of  $\gamma_1^1$  it might happen that  $e''_{11}$  does not exist; in this case define  $e''_{11}$  as a virtual edge that links  $\gamma_1^1$  to  $z_3^{2n}$ , where  $2n$  is the number of vertices of the  $J^2$ -gem); let  $v$  be the intersection of the line  $x = x_i^j$  and the edge  $e'_{ij}$ ; let  $w$  be the intersection of the line  $x = x_i^j$  and the edge  $e''_{ij}$ ;  $z_i^j \leftarrow (v + w)/2$ ; UNTIL  $j = \text{length of } \gamma_i$ ; UNTIL  $i = k$ ; END.

We apply the algorithms of the previous two figures to obtain a rectilinear embedding of  $\mathcal{W}$  in linear time. The connection between  $\mathcal{W}$ ,  $\mathcal{W}_1^\circ$  and  $\mathcal{H}_1^\circ$  is explained in Figure 18.

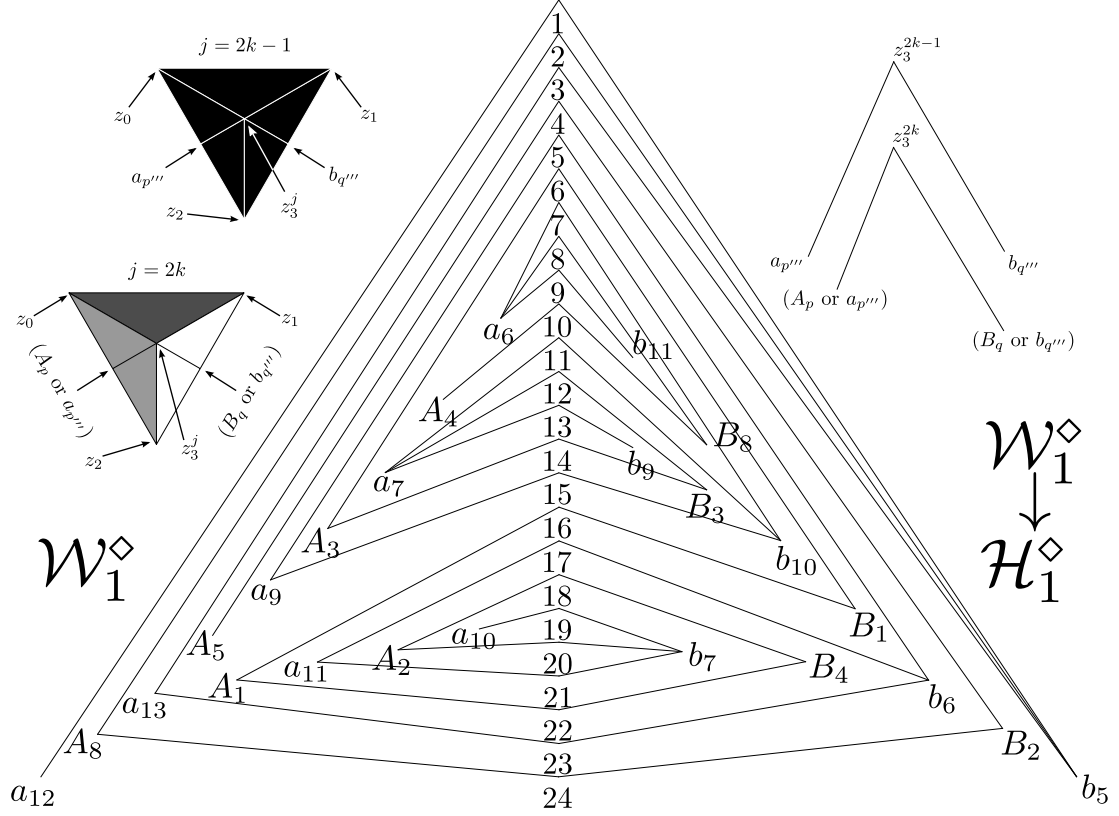


Figure 18: To get  $\mathcal{W}_1^\diamond = \mathcal{W}_1^{\diamond'} \cup \mathcal{W}_1^{\diamond''}$  from  $\mathcal{W}$  remove all but two straight line segments emanating from  $z_3^k$ , one in each side. The two segments that survive are the ones finishing at the smallest index upper case  $A_p$  (when there is a choice) and the smallest indexed upper case  $B_q$  (when there is a choice). Let  $\{x\} \cup Y \subseteq \mathbb{R}^N$ , for  $1 \leq N \in \mathbb{N}$ . The *cone* [15] with vertex  $x$  and base  $Y$ , denoted  $x * Y \subseteq \mathbb{R}^N$ , is the union of  $Y$  with all line segments which link  $x$  to  $y \in Y$ . The passage  $\mathcal{W}_1^\diamond \rightarrow \mathcal{H}_1^\diamond$  is straightforward by a cone algorithm: for each  $e' \in \mathcal{W}_1^{\diamond'}$  add the two 2-simplices  $z_0 * e'$  and  $z_2 * e'$  to  $\mathcal{H}_1^\diamond$ ; for each  $e'' \in \mathcal{W}_1^{\diamond''}$  add the two 2-simplices  $z_1 * e''$  and  $z_2 * e''$  to  $\mathcal{H}_1^\diamond$ . To complete  $\mathcal{H}_1^\diamond$  add the 2-simplices  $\{z_3^j z_1 z_0 \mid j = 1, \dots, 2n\}$ .

## 2.4 Fourth phase: filling the pillows, to obtain the PL-embedding of $\mathcal{H}^*$ we seek: $\mathcal{H}_1^\diamond, \mathcal{H}_2^\diamond, \dots, \mathcal{H}_{n-1}^\diamond, \mathcal{H}_n^\diamond = \mathcal{H}^*$

We start the fourth phase with  $\mathcal{W}_1^\diamond$  and  $\mathcal{H}_1^\diamond$ , which is defined in Fig. 18.

**(2.7) Proposition.** *If  $\mathcal{W}_1^\diamond$  is embedded rectilinearly in  $\Pi' \cup \Pi''$ , then it can be extended to an embedding of  $\mathcal{H}_1^\diamond$  into  $\mathbb{R}^3$ , via the cone construction.*

**Proof.** Straightforward from the simple geometry of the situation. See Fig. 18. □

Let  $\mathcal{L}_{i+1}^*$  be a subset of the pillow  $\mathcal{P}_{i+1}^*$ , formed by the part that comes from the tail of the balloon after the  $i$ -th  $bp$ -move is applied, see Fig. 19.

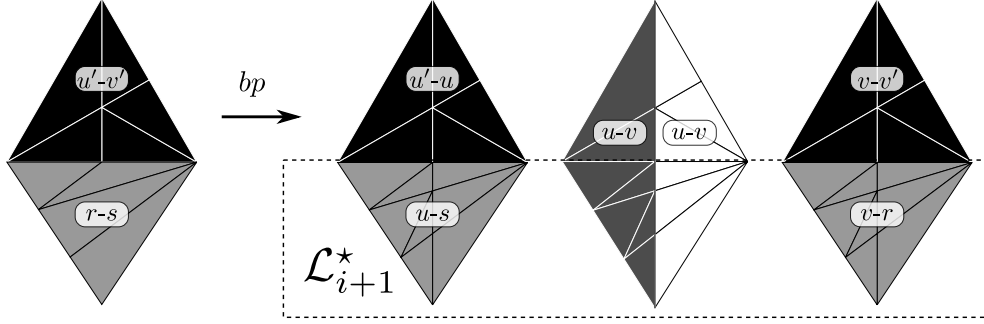


Figure 19: The set  $\mathcal{L}_{i+1}^*$ 's: at each step of Theorem 2.8 we embed a set  $\mathcal{L}_{i+1}^*$ ,  $i = 0, \dots, n-1$  of 2-simplices. These sets are the complementary parts of the PL2-faces already in  $\mathcal{H}_1^\circ$  after a change of colors in the medial layer. The process of replacing the combinatorial tail of a balloon by the corresponding trio of embedded PL2-faces in the pillow is denominated *the blowing up of the balloon's tail*.

**(2.8) Theorem.** *There is an  $O(n)$ -algorithm for blowing up a single balloon's tail. Thus finding  $\mathcal{H}_n^*$  take,  $O(n^2)$  steps.*

**Proof.**  $\mathcal{H}_{i+1}^\circ$  is the union of  $\mathcal{H}_i^\circ$  with  $\mathcal{L}_{i+1}^*$  and an  $\epsilon$ -change in some PL3-faces, if the rank of the type of balloon's tail of the  $i$ -th  $bp$ -move has rank greater than 1 (we call  $\epsilon$ -change because this change is small, as described below). At the same time we update the colors of the middle layer to match the colors of the  $i$ -th pillow in the sequence of  $bp$ -moves.

Now we describe how to embed each kind of  $\mathcal{L}_i^*$  (explaining how to  $\epsilon$ -change some PL3-faces, to get space for  $E\mathcal{L}_i^*$ ).

If the balloon's tail is of type  $P_1$  (the case  $B_1$  is analogous). Make two copies of  $P_1$ , resulting in three  $P_1$ , but change the color of the one which will be in the middle, and define the 0-simplices like in Fig. 20.

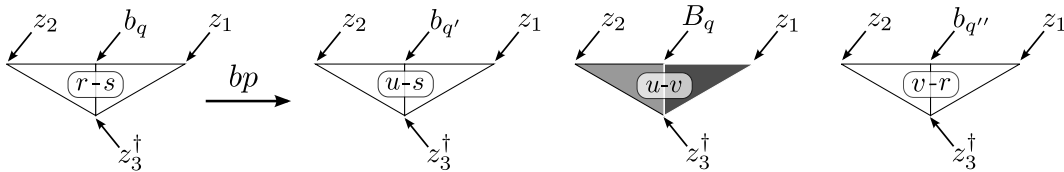


Figure 20: Embedding the part of the pillow corresponding to the tail of the balloon: case  $P_1$  of the tail.

If the balloon's tail is of type  $B_i$ ,  $i > 1$  (the case  $P_i$  is analogous). Make two copies of  $B_i$ , refine the copies and the original, resulting in three  $B_i'$ , but change the color of the one which will be in the middle, and define the 0-simplices like in Fig. 21.

The images  $\chi_j$  we already know from previous  $bp$ -move, now we need to define all the images  $\alpha_j, \beta_j$  and  $\gamma_j$ . Let  $\beta_j$  be  $\frac{z_2 + \chi_{j+1}}{2}$  for each  $j = 1, \dots, i$ . As the images  $\alpha_j$  and  $\gamma_j$  can be defined in analogous way, we just explain how to define each  $\alpha_j$ . We know that each  $\alpha_j$  is in the PL3-face  $\nabla_r$ . To define each  $\alpha_j$  we need to reduce the PL3-face  $\nabla_r$  in order to get enough space for the PL2-faces of color 0 and 2 of the PL3-faces  $\nabla_u$  and  $\nabla_v$ . Consider the PL3-face  $\nabla_r$ , each  $\beta_j$  is

already defined, so define each  $\zeta_j$  as  $\frac{z_2 + \omega_{j+1}}{2}$ , where  $\omega_k$  is previously defined, see Fig. 22. Define  $\alpha_j$  as  $\frac{\zeta_j + \beta_j}{2}$ .

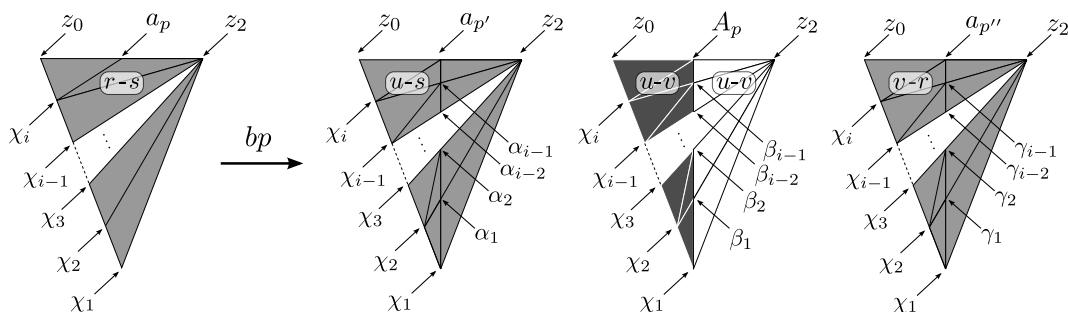


Figure 21: Embedding the part of the pillow corresponding to the tail of the balloon: case  $B_i$  of the tail.

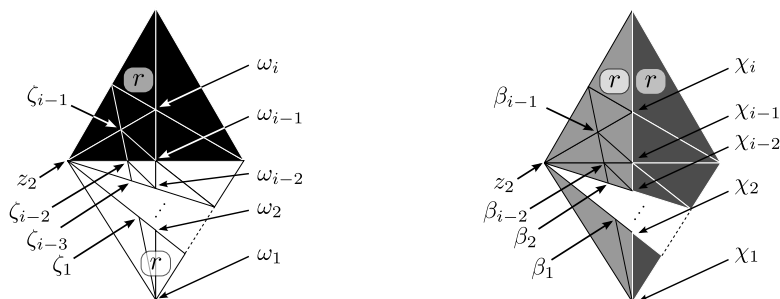


Figure 22: Using the PL3-face corresponding to  $r$  to define the  $\alpha_j$  as  $\frac{\zeta_j + \beta_j}{2}$ .

The last case is when balloon's tail is refined, that means it is of type  $P'_i$  or  $B'_i$ ,  $i > 1$ . We treat the case  $B'_i$ , see Fig. 23. All the 0-simplices  $\beta_j$  are already defined, we need to define each  $\alpha_j$  and each  $\gamma_j$ . Observe that here  $r \neq s - 1$  and the definitions of  $\alpha_j$  and  $\gamma_j$  are not analogous.

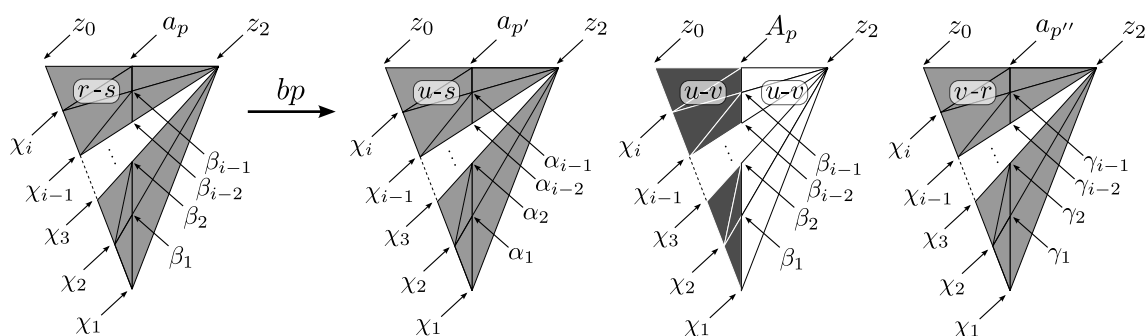


Figure 23: Embedding the part of the pillow corresponding to the tail of the balloon: case  $B'_i$  of the tail.

In this case, we need to reduce the PL3-faces  $\nabla_r$  and  $\nabla_s$  to create enough space to build PL2-faces 0- and 2-colored. To define 0-simplices  $\alpha_j$  and  $\gamma_j$ , one of these cases is analogous to the

case not refined, but the other we describe here. ( $\nabla_r$  in the new case is the rank of PL $2_0$ -face is equals to the rank of the PL $2_1$ -face plus 2, if its not true, the new case is in the PL3-face  $\nabla_v$ ). Suppose that the new case is in the PL3-face,  $\nabla_r$ . To define  $\alpha_j$ , suppose that the PL $2_0$ -face of this PL3-face is not refined, see Fig. 24. Define each  $\alpha_j$  as the middle point between  $\beta_j$  and  $\omega_j$ .

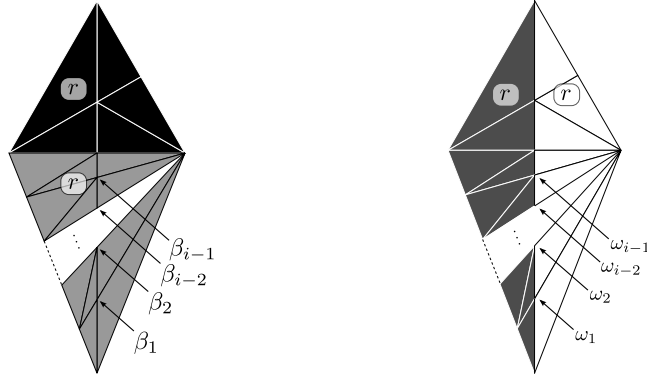


Figure 24: Using the PL3-face  $\nabla_r$  to define  $\alpha_j$  as  $\frac{\omega_j + \beta_j}{2}$ .

Consider the case that the PL $2_0$ -face, of the PL3-face  $\nabla_r$ , is refined see Fig. 25. This is a final subtlety which is treated with the *bump*. This is characterized by a non-convex pentagon shown in the bottom part of Fig. 25. Let  $\nu_j$  be  $\frac{z_2 + \omega_j}{2}$  and  $\alpha_j$  as  $\frac{\beta_{j-1} + \nu_j}{2}$ , for  $j = 1, \dots, i-1$ . Observe that if we define  $\alpha_j$  as if the PL $2_0$ -face where not refined, some 1-simplices may cross.

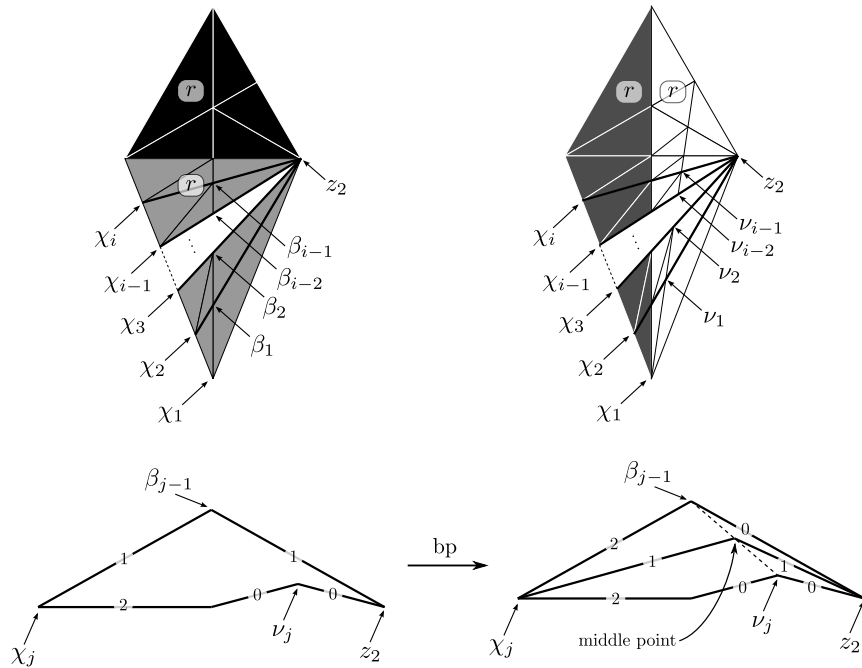


Figure 25: The bump: a final subtlety and how to deal with it.

□

## References

- [1] É. Colin de Verdière, M. Pocchiola, and G. Vegter. Tutte’s barycenter method applied to isotopies. *Computational Geometry*, 26(1):81–97, 2003.
- [2] Thomas H Cormen, Charles E Leiserson, Ronald L Rivest, and Clifford Stein. *Introduction to Algorithms*. MIT press, 2001.
- [3] M. Ferri and C. Gagliardi. Crystallisation moves. *Pacific J. Math*, 100(1):85–103, 1982.
- [4] L. D. Lins. Blink: a language to view, recognize, classify and manipulate 3D-spaces. <http://arxiv.org/arXiv:math/0702057>, 2007.
- [5] S. Lins. A simple proof of Gagliardi’s handle recognition theorem. *Discrete mathematics*, 57(3):253–260, 1985.
- [6] S. Lins. On the fundamental group of 3-gems and a planar class of 3-manifolds. *European Journal of Combinatorics*, 9(4):291–305, 1988.
- [7] S. Lins and A. Mandel. Graph-encoded 3-manifolds. *Discrete Math.*, 57(3):261–284, 1985.
- [8] S. Lins and M. Mulazzani. Blobs and flips on gems. *Journal of Knot Theory and its Ramifications*, 15(8):1001–1035, 2006.
- [9] S. L. Lins. *Gems, Computers, and Attractors for 3-Manifolds*. World Scientific, 1995.
- [10] S. L. Lins. Closed oriented 3-manifolds are equivalence classes of plane graphs. <http://arxiv.org/abs/1305.4540>, 2013.
- [11] S. L. Lins and L. D. Lins. All the shapes of spaces: a census of small 3-manifolds. <http://arxiv.org/abs/1305.5590>, 2013.
- [12] S. L. Lins and R. N. Machado. Framed link presentations of 3-manifolds by an  $O(n^2)$  algorithm, I: gems and their duals. *arXiv:1211.1953v2 [math.GT]*, 2012.
- [13] S. L. Lins and R. N. Machado. Framed link presentations of 3-manifolds by an  $O(n^2)$  algorithm, II: colored complexes and boundings in their complexity. *arXiv:1212.0826v2 [math.GT]*, 2012.
- [14] S. L. Lins and R. N. Machado. Framed link presentations of 3-manifolds by an  $O(n^2)$  algorithm, III: geometric complex  $\mathcal{H}_n^*$  embedded into  $\mathbb{R}^3$ . *arXiv:1212.0827v2 [math.GT]*, 2012.
- [15] C.P. Rourke and B.J. Sanderson. *Introduction to piecewise-linear topology*, volume 69. Springer-Verlag, 1982.
- [16] J. Stillwell. *Classical Topology and Combinatorial Group Theory*. Springer Verlag, 1993.
- [17] W. T. Tutte. How to draw a graph. *Proc. London Math. Soc.*, 13(3):743–768, 1963.

Sóstenes L. Lins  
Centro de Informática, UFPE  
Av. Jornalista Aníbal Fernandes s/n  
Recife-PE 50740-560  
Brazil  
sostenes@cin.ufpe.br

Ricardo N. Machado  
Núcleo de Formação de Docentes, UFPE  
Av. Jornalista Aníbal Fernandes s/n  
Caruaru-PE  
Brazil  
ricardonmachado@gmail.com